Circulation

ORIGINAL RESEARCH ARTICLE

Novel Long Noncoding RNA *HEAT4* Affects Monocyte Subtypes, Reducing Inflammation and Promoting Vascular Healing

Jasmin M. Kneuer, MS; Ignacy A. Grajek; Melanie Winkler; Stephan Erbe, MS; Tim Meinecke, MD; Ronald Weiss, PhD; Tania Garfias-Veitl, PhD; Bilal N. Sheikh, PhD; Ann-Christine König, PhD; Maximilian N. Möbius-Winkler, MD; Alexander Kogel, MD; Karl-Patrik Kresoja, MD; Sebastian Rosch, MD; Karoline E. Kokot, PhD; Vanina Filipova; Susanne Gaul, PhD; Holger Thiele, MD; Philipp Lurz, MD, PhD; Stephan von Haehling, MD, PhD; Thimoteus Speer, MD, PhD; Ulrich Laufs, MD; Jes-Niels Boeckel, PhD

BACKGROUND: Activation of the immune system contributes to cardiovascular diseases. The role of human-specific long noncoding RNAs in cardioimmunology is poorly understood.

METHODS: Single-cell sequencing in peripheral blood mononuclear cells revealed a novel human-specific long noncoding RNA called *HEAT4* (heart failure–associated transcript 4). *HEAT4* expression was assessed in several in vitro and ex vivo models of immune cell activation, as well as in the blood of patients with heart failure (HF), acute myocardial infarction, or cardiogenic shock. The transcriptional regulation of *HEAT4* was verified through cytokine treatment and single-cell sequencing. Loss-of-function and gain-of-function studies and multiple RNA–protein interaction assays uncovered a mechanistic role of *HEAT4* in the monocyte anti-inflammatory gene program. *HEAT4* expression and function was characterized in a vascular injury model in NOD.CB17-Prkdc scid/Rj mice.

RESULTS: *HEAT4* expression was increased in the blood of patients with HF, acute myocardial infarction, or cardiogenic shock. *HEAT4* levels distinguished patients with HF from people without HF and predicted all-cause mortality in a cohort of patients with HF over 7 years of follow-up. Monocytes, particularly anti-inflammatory CD16$^+$ monocytes, which are increased in patients with HF, are the primary source of *HEAT4* expression in the blood. *HEAT4* is transcriptionally activated by treatment with anti-inflammatory interleukin-10. *HEAT4* activates anti-inflammatory and inhibits proinflammatory gene expression. Increased *HEAT4* levels result in a shift toward more CD16$^+$ monocytes. *HEAT4* binds to S100A9, causing a monocyte subtype switch, thereby reducing inflammation. As a result, *HEAT4* improves endothelial barrier integrity during inflammation and promotes vascular healing after injury in mice.

CONCLUSIONS: These results characterize a novel endogenous anti-inflammatory pathway that involves the conversion of monocyte subtypes into anti-inflammatory CD16$^+$ monocytes. The data identify a novel function for the class of long noncoding RNAs by preventing protein secretion and suggest long noncoding RNAs as potential targets for interventions in the field of cardioimmunology.

Key Words: heart failure ■ monocytes ■ regeneration ■ RNA, long noncoding

Correspondence to: Jes-Niels Boeckel, PhD, Klinik und Poliklinik für Kardiologie, Universitätsklinikum Leipzig, Johannisallee 30, 04103 Leipzig, Germany. Email boeckel@medizin.uni-leipzig.de

Supplemental Material is available at https://www.ahajournals.org/doi/suppl/10.1161/CIRCULATIONAHA.124.069315.
For Sources of Funding and Disclosures, see page XXX.

Circulation is available at www.ahajournals.org/journal/circ

ORIGINAL RESEARCH ARTICLE

Clinical Perspective

What Is New?

- *HEAT4* (heart failure–associated transcript 4) is a novel human-specific long noncoding RNA that is enriched in monocytes and induced in patients with heart failure, acute myocardial infarction, or cardiogenic shock.
- *HEAT4* levels can distinguish patients with heart failure from people without heart failure and are predictive of all-cause mortality in a cohort of patients with heart failure over 7 years of follow-up.
- *HEAT4* promotes an anti-inflammatory monocytic CD16$^+$ cell phenotype and exacerbates injury-induced vascular healing, which involves *HEAT4* physical interaction with S100A9, thereby preventing its secretion and promoting its translocation to the nucleus, where it binds to promoter regions.

What Are the Clinical Implications?

- Our findings provide new insight into therapeutic strategies for cardiovascular disease by targeting the interplay between coding and noncoding pathways.
- Targeting long noncoding RNAs may represent an approach to control monocyte-mediated inflammation.

Nonstandard Abbreviations and Acronyms

CANTOS	Canakinumab Anti-Inflammatory Thrombosis Outcomes Study
CVD	cardiovascular disease
HEAT3	heart failure–associated transcript 3
HEAT4	heart failure–associated transcript 4
HEK	human embryonic kidney
HF	heart failure
IL	interleukin
ITGAM	integrin alpha M
lncRNA	long noncoding RNA
MI	myocardial infarction
PBMC	peripheral blood mononuclear cell
PREDICT-HFpEF	Prediction of the Development of Heart Failure With Preserved Ejection Fraction
PRIDE	Proteomics Identifications
qPCR	quantitative polymerase chain reaction
RNA-seq	next-generation bulk RNA sequencing
scRNA-seq	single-cell RNA sequencing
SHOCK-COOL	Mild Hypothermia in Cardiogenic Shock Complicating Myocardial Infarction
SICA-HF	Studies Investigating Comorbidities Aggravating Heart Failure
TNFα	tumor necrosis factor α

The immune system plays a crucial role in maintaining human health by protecting against invading pathogens and foreign substances. Dysregulations of the immune system contribute to the development and progression of various human diseases, including cancer,[1,2] autoimmune disorders,[3,4] and cardiovascular diseases (CVDs).[5,6]

The inflammatory process has anti-inflammatory and proinflammatory phases, which are characterized by changes in inflammatory cytokines and immune cell types.[7] These cells and signaling molecules are temporarily activated and deactivated in a temporal sequence of an inflammatory and a healing phase. Prolonged and pathologic activation of inflammatory cell types and signaling molecules, such as interleukin (IL)–6 or IL-1β, can cause chronic disease states, such as heart failure (HF) and atherosclerosis.[8–10] Anti-inflammatory interventions (eg, inhibition of IL-1β in CANTOS [Canakinumab Anti-Inflammatory Thrombosis Outcomes Study]) exert beneficial effects on CVD outcomes.[11,12] However, transient activation of components of both pro-inflammatory and anti-inflammatory pathways are important for regenerative processes (eg, vascular healing after ischemia and reperfusion). Prolonged activation of anti-inflammatory processes is associated with negative effects in chronic HF as well.[13–15] Therefore, a better understanding of the cellular and molecular basis of anti-inflammatory processes is necessary to develop more effective strategies to diagnose and potentially control the inflammatory process in CVDs.

Inflammatory cells, including monocytes and T cells, infiltrate the heart after myocardial injury and can clear damaged tissue. However, excessive or prolonged inflammation can lead to the development of fibrosis and hypertrophy, conditions that are associated with impaired cardiac function.[16–18] Monocytes are the primary participants in early inflammation, with different subsets exhibiting both pro-inflammatory and anti-inflammatory functions within the inflammatory process.[19] Different subsets can be distinguished on the basis of their expression of CD16. CD16$^+$ monocytes patrol the vasculature, do not infiltrate, and are implicated in the anti-inflammatory part of the inflammatory process.[20] Gaining a deeper understanding of monocyte subtype transitions in humans has the potential to unlock novel therapeutic options for treating inflammation, including in CVDs.

Rapid transcriptional regulation is a key aspect of gene expression control within the immune system, and emerging evidence highlights the important role of long noncoding RNAs (lncRNAs) in this process.[21] LncRNAs have recently garnered increasing attention as critical modulators of various biologic processes.[22] These versatile molecules exhibit distinct expression patterns specific to different immune cell lineages and play pivotal roles in governing the differentiation and functions of both innate and adaptive cell populations.[23–26] LncRNAs were recently shown to be important regulators of inflammation and fibrosis in cardiovascular cell types, such as vascular smooth muscle cells (SMCs) and fibroblasts, in the cardiovascular system.[27,28] Unraveling the intricate mechanisms through which lncRNAs contribute to immune cell regulation can provide valuable insights into the transcriptional control within the immune system.

In this study, an unbiased single-cell sequencing approach revealed a novel human-specific lncRNA named *HEAT4* (heart failure–associated transcript 4). *HEAT4* levels were increased in the blood of patients with HF, acute myocardial infarction (MI), or cardiogenic shock. We show that *HEAT4* is enriched in anti-inflammatory CD16$^+$ monocytes and activates anti-inflammatory and inhibits proinflammatory gene expression. Increased *HEAT4* levels result in a shift toward more CD16$^+$ monocytes. The lncRNA *HEAT4* was discovered to be able to bind to the S100A9 protein. This mechanism prevents secretion of the S100A8/A9 heterodimer. Using a humanized mouse model, we observed that *HEAT4*-expressing monocytes promoted vascular healing after carotid artery injury. These data identify a novel mechanism that controls the human monocyte subpopulation by a human-specific lncRNA modifying inflammation in human disease.

METHODS

Patient Inclusion

Cohort 1

Patient inclusion in this study was approved by the ethics committee at the University of Leipzig (approval 416/18-ek). The study was conducted in accordance with the Declaration of Helsinki. All participants gave written informed consent for molecular analysis. The HF group included patients with clinically stable HF with reduced ejection fraction (ie, left ventricular ejection fraction ≤40%) of ischemic origin defined according to the European Society of Cardiology.[29] Patients with relevant valvular heart disease (eg, moderate or greater stenosis or regurgitation) were excluded. Patients with a history of myocarditis, regular alcohol consumption, illicit drug use, cardiotoxic chemotherapy, or unclear pathogenesis of HF were excluded. Patients with normal left ventricular ejection fraction without signs or symptoms of HF, normal natriuretic peptide levels, and no evidence of structural cardiac alterations served as controls. Those patients were recruited from the prospective ongoing cohort study PREDICT-HFpEF (Prediction of the Development of Heart Failure With Preserved Ejection Fraction; URL: https://www.clinicaltrials.gov; Unique identifier: NCT04894968) at Heart Center Leipzig and as part of 008/20-ek at University Hospital Leipzig.

Cohort 2

Next-generation bulk RNA sequencing (RNA-seq) data of peripheral blood mononuclear cells (PBMCs) from 4 patients with ischemic cardiomyopathy and 4 controls published as cohort 2 in reference [24] were used.

Cohort 3

Quantitative polymerase chain reaction (qPCR) of RNA isolated from whole blood samples from 38 controls and 63 patients with HF was performed. Patients were enrolled as part of SICA-HF (Studies Investigating Comorbidities Aggravating Heart Failure) between February 2010 and March 2014.[30,31] Participants were followed for >7 years (mean follow-up time, 2701±998 days) until the database was censored in August 2018.

Cohort 4

qPCR of RNA isolated from PBMCs from 23 controls and 43 patients with acute MI (part of a recently published cohort of patients with acute MI[32]) was performed.

Cohort 5

qPCR of RNA isolated from whole blood samples from 5 controls and 4 patients with cardiogenic shock was performed. Controls are part of a recently published control group[33] and patients with cardiogenic shock are part of the recently published randomized SHOCK-COOL trial (Mild Hypothermia in Cardiogenic Shock Complicating Myocardial Infarction).[34]

Carotid Injury Model

Ten-week-old male NOD.CB17-Prkdc scid/Rj mice were anesthetized with isoflurane and the left common carotid artery was injured. CD14$^+$ human monocytes were injected through the retrobulbar venous plexus. After 3 days, Evans blue was injected, and mice were killed 1 hour later. The left carotid arteries were excised and analyzed. All animal experiments were approved by the Veterinary Office of Saarland, Germany (approval 34/2014).

Statistical Analysis and Blinding

GraphPad Prism 8 and IBM SPSS Statistics (version 29.0.0 [241]) were used for statistical analysis. Outliers were excluded and columns were tested for normality. When 2 groups were compared, paired and unpaired (with Welch correction if no equal SDs were assumed) *t* tests were used for Gaussian distributed values. For non-Gaussian distributed values, Wilcoxon matched-pairs signed rank test was used for paired experiments and Mann-Whitney test for unpaired experiments. Comparisons of >2 groups were performed with 1-way or 2-way ANOVA. For 1-way ANOVA, paired Gaussian-distributed values were analyzed by repeated measures or mixed model 1-way ANOVA, both followed by Dunnett multiple comparisons; paired non-Gaussian distributed values by Friedman test followed by Dunn multiple comparison test; and unpaired non-Gaussian distributed values by Kruskal-Wallis followed

ORIGINAL RESEARCH ARTICLE

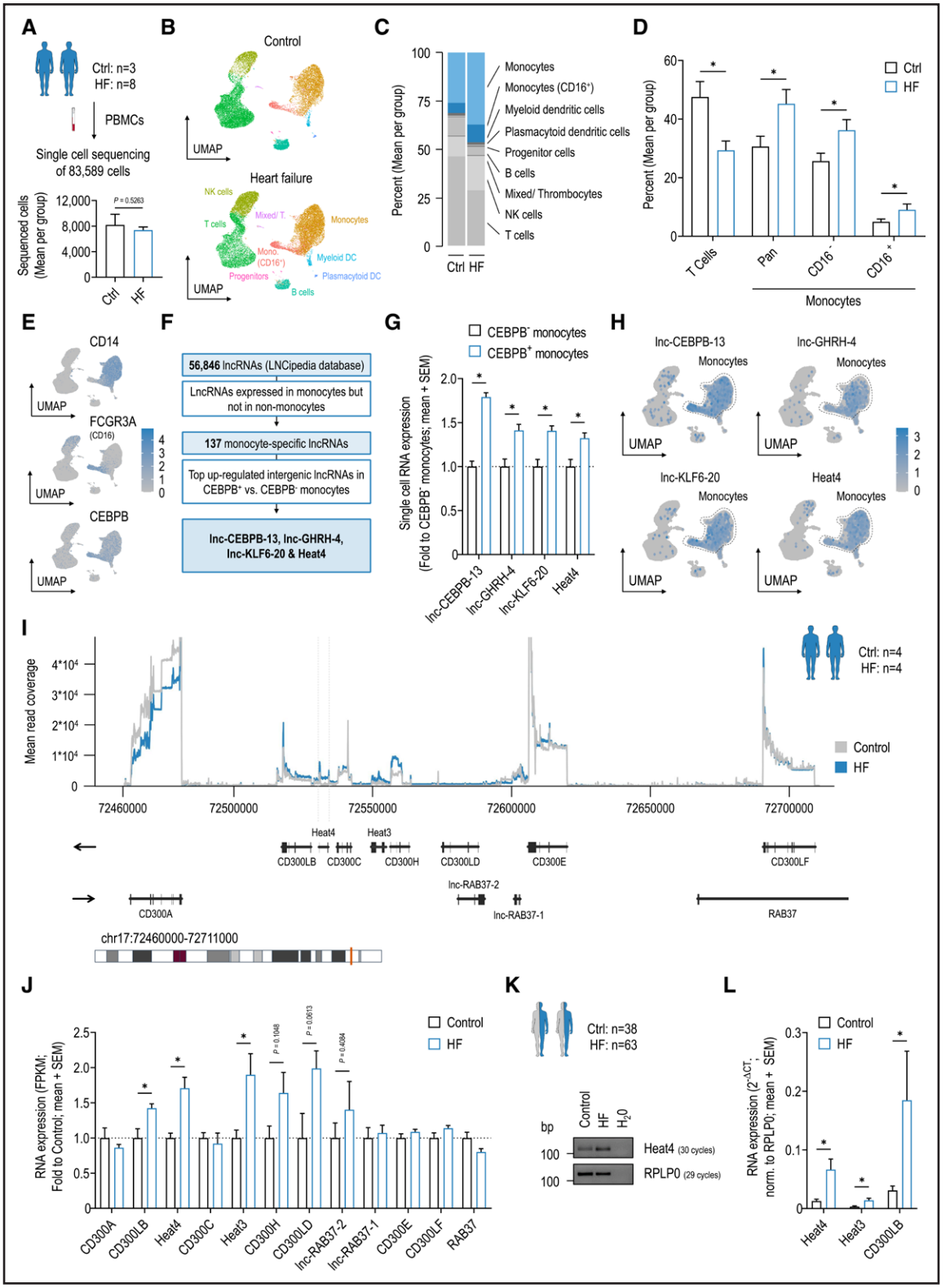

Figure 1. Characterization of peripheral immune cell populations altered in patients with heart failure and identification of altered HEAT4 expression.

A, Schematic illustration of single-cell RNA sequencing. Peripheral blood mononuclear cells (PBMCs) are isolated from blood samples drawn from controls (n=3) and patients with heart failure (HF; n=8; cohort 1), then subjected to single-cell RNA sequencing. Sequenced cells are presented as mean per group (controls, n=3; HF, n=8; 2-tailed unpaired *t* test). **B**, Uniform manifold approximation and projection (UMAP) plots showing the final annotation of single cell clusters to immune cell types in PBMCs from controls and patients with HF. A total of 20 000 randomly selected cells per condition are shown for comparability. **C**, Percentages of the annotated cell types are shown as mean for each group. (*Continued*)

Figure 1 Continued. **D**, The percentage of T cells, all monocytes, and the monocyte subtypes CD16⁻ and CD16⁺ in controls and patients with HF, shown as mean per group (controls, n=3; HF, n=8; 2-tailed unpaired *t* tests with Welch correction). **E**, Cell type–specific expression of *CD14*, *FCGR3A* (CD16), and *CEBPB* according to (**B**). **F**, Single-cell RNA sequencing data obtained from PBMCs from controls and patients with HF are analyzed for the expression of 56 846 long noncoding RNAs (lncRNAs) included in the LNCipedia database. The analysis identified 137 lncRNAs that are specifically expressed in monocytes, among which lnc-*CEBPB*-13, lnc-*GHRH*-4, lnc-*KLF6*-20, and *HEAT4* (heart failure–associated transcript 4) are the top upregulated lncRNAs in CEBPB⁺ vs CEBPB⁻ monocytes. **G**, Relative expressions of lnc-*CEBPB*-13, lnc-*GHRH*-4, lnc-*KLF6*-20, and *HEAT4* in CEBPB⁺ vs CEBPB⁻ monocytes based on the single-cell RNA sequencing data (CEBPB⁻, n=12 224; CEBPB⁺, n=22 932; 2-tailed Mann-Whitney tests). **H**, Cell type–specific expression of genes shown in **F** and **G** according to **B** in PBMCs from all samples together (controls+patients with HF; n=11). **I**, Mean read coverage of genes located on chromosome 17 between base pairs 72460000 and 72711000 (hg19) detected by next-generation bulk RNA sequencing in PBMCs from controls (n=4) and patients with HF (n=4; cohort 2) shown as track plot. Locations of the genes on the forward (arrow pointing right; →) or reverse strand (arrow pointing left; ←) and the idiogram of chromosome 17 are shown below. **J**, RNA expression of the genes located on chromosome 17 base pairs 72460000 to 72711000 in patients with HF (n=4) relative to controls (n=4; 2-tailed unpaired *t* tests). **K**, Agarose gels showing the levels of *HEAT4* and *RPLP0*, which was used as a reference gene, in 2 representative patients from cohort 3. Thirty quantitative polymerase chain reaction cycles were used for *HEAT4* and 29 for *RPLP0*. **L**, RNA levels of *HEAT3* (heart failure–associated transcript 3), *HEAT4*, and *CD300LB* determined by quantitative reverse transcription polymerase chain reaction in whole blood samples from the sex-mixed validation cohort (cohort 3) of controls (n=38) and patients with HF (n=63; 2-tailed Mann-Whitney tests). Bar graphs are presented as mean+SEM. Statistical differences were calculated using Mann-Whitney test or unpaired *t* test with or without Welch correction (*P<0.05).

by Benjamini-Krieger-Yekutieli test. For 2-way ANOVA, values were analyzed by ordinary 2-way ANOVA followed by Tukey multiple comparisons test. Survival curves were compared using Mantel-Cox log-rank test. P<0.05 was considered significant.

For animal experiments, mice were randomly divided within blocks into treatment and control groups. Blinding procedures to mask group and treatment assignment were used to ensure that the experimenter was unaware of the treatment allocation. See the extended Methods in the Supplemental Material for further description.

Data Availability

The single-cell RNA-seq (scRNA-seq), bulk RNA sequencing, and chromatin immunoprecipitation sequencing data sets shown in this publication can be accessed at the National Center for Biotechnology Information Gene Expression Omnibus[35] with accession number GSE267646. The mass spectrometry proteomics data have been deposited to the ProteomeXchange Consortium through the PRIDE (Proteomics Identifications)[36] partner repository with dataset identifier PXD052076.

RESULTS

Characterization of Peripheral Immune Cell Populations Altered in HF and Identification of Altered *HEAT4* Expression

To characterize the peripheral immune cell populations in patients with HF, scRNA-seq of equal numbers of PBMCs obtained from 8 patients with HF and 3 controls (cohort 1; Figure 1A; Table S1) was conducted. Data integration from the resulting 83 589 cells identified 15 distinct clusters (Figure S1A). Cell types were assigned to these clusters on the basis of established markers,[37] as well as results from the SingleR tool[38] (eg, using CD14 and CD16 for monocytes, CD79A for B cells, and CD3E for T cells; Figure 1B; Figure S1B through S1F). The resulting cell type annotations revealed a decrease in the proportion of T cells, an increase in the proportion of monocytes, and a higher proportion of CD16⁺ monocytes in patients with HF compared with controls (Figure 1C and 1D; Figure S1G and S1H). Next, we aimed to simultaneously identify lncRNAs and mRNAs associated with the altered immune cell composition toward more CD16⁺ monocytes in patients with HF. Therefore, a custom reference genome consisting of a combination of the standard human reference genome (hg38) and the annotation of 56 846 lncRNAs (LNCipedia) was created. In the search for transcripts that can induce the expression of CD16 (FCGR3A) in monocytes, we filtered on the basis of the expression of CEBPB, a relevant factor for the number and survival of CD16⁺ monocytes,[39] rather than relying on the presence of CD16 expression (Figure 1E).

This analysis revealed 4 intergenic lncRNAs to be top-enriched in the CEBPB⁺ versus CEBPB⁻ monocytes population: lnc-*CEBPB*-13, lnc-*GHRH*-4, lnc-*KLF6*-20, and *HEAT4* (Figure 1F through 1H; Table S2). The lncRNA *HEAT4* is expressed from a gene within the *CD300* gene cluster, which includes 8 protein-coding genes that encode 7 members of the *CD300* family of cell surface receptors and a non-*CD300* family protein. The *CD300* gene cluster also encodes for several uncharacterized lncRNAs, including *HEAT3* (heart failure–associated transcript 3) and *HEAT4* (Figure 1I). The *CD300* family receptors are predominantly expressed on immune cells and have crucial roles in modulating immune responses, such as activating, inhibiting, and regulating various immune cell functions.[40] To further investigate the association of these RNAs with HF and to analyze lncRNA expression with high sequencing depth, next-generation bulk RNA-seq analysis was performed on PBMCs from 4 patients with HF and 4 controls (cohort 2), and showed increased expression levels of *CD300LB*, *HEAT3*, and *HEAT4* in patients with HF; other genes encoded within the *CD300* gene clusters were not significantly altered (Figure 1I and 1J). These findings were validated in a larger independent cohort (cohort 3: controls, n=38; HF, n=63; Table S3), and found *HEAT4* to be the most strongly induced lncRNA in patients with HF (Figure 1K and 1L).

ORIGINAL RESEARCH ARTICLE

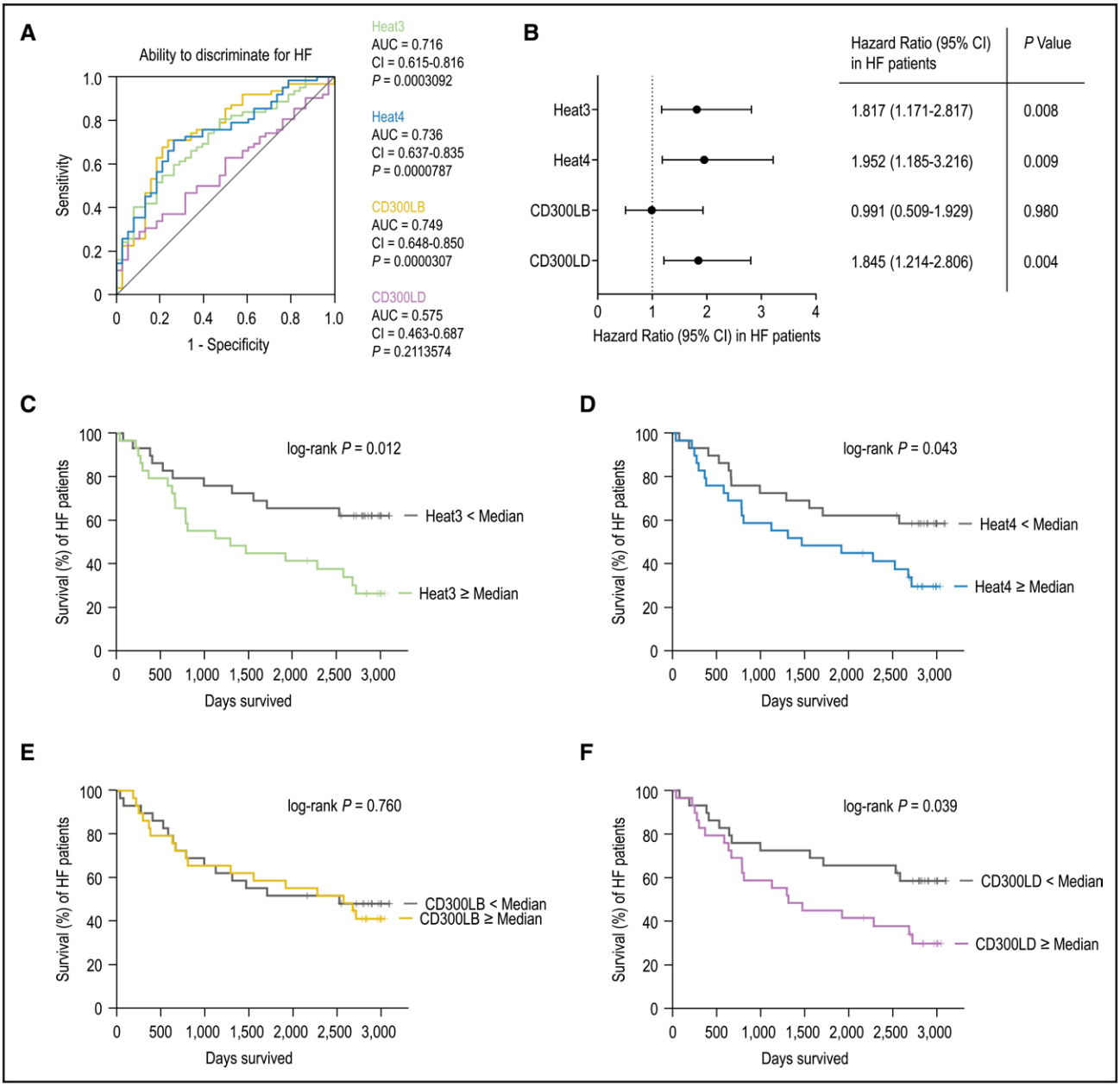

Figure 2. Association of HEAT3, HEAT4, CD300LB, and CD300LD with incidence and survival in heart failure.
A, Area under the receiver operating characteristic (AUC) curve for *HEAT3* (heart failure–associated transcript 3), *HEAT4* (heart failure–associated transcript 4), *CD300LB*, and *CD300LD* level using a univariate model demonstrating the discriminatory ability of each RNA between controls (n=38) and patients with heart failure (HF; n=63, cohort 3). **B**, The relationship between survival time and *HEAT3*, *HEAT4*, *CD300LB*, and *CD300LD* level as continuous predictor variables using a Cox proportional hazards analysis (univariate model) indicates the all-cause mortality risk as hazard ratio (HR). Participants (cohort 3) were followed for >7 years (mean follow-up time, 2701±998 days) until the database was censored. Kaplan-Meier curves visualize the probability of survival into 2 groups of patients with HF with lower or higher RNA expression of *HEAT3* (median, 0.0025; **C**), *HEAT4* (median, 0.0169; **D**), *CD300LB* (median, 0.0506; **E**) and *CD300LD* (median, 0.0185; **F**), each divided by their median. Comparisons of the 2 survival curves were assessed by Mantel-Cox log-rank test.

Next, we investigated the clinical relevance of the RNAs encoded by the *CD300* gene cluster that are regulated in patients with HF, such as *HEAT3*, *HEAT4*, *CD300LB*, and *CD300LD*, which failed statistical difference (P=0.06), by examining whether these RNA expression levels measured in whole blood have the ability to discriminate patients with HF from controls and are predictors of survival. *HEAT3*, *HEAT4*, and *CD300LB* levels obtained from whole blood samples collected from cohort 3 (controls, n=38 [deceased, n=0]; HF, n=63 [deceased, n=32]; 7-year follow-up; Table S3) demonstrated a significant discriminatory ability for HF. The area under the receiver operating characteristic curve was 0.716, 0.736, and 0.749,

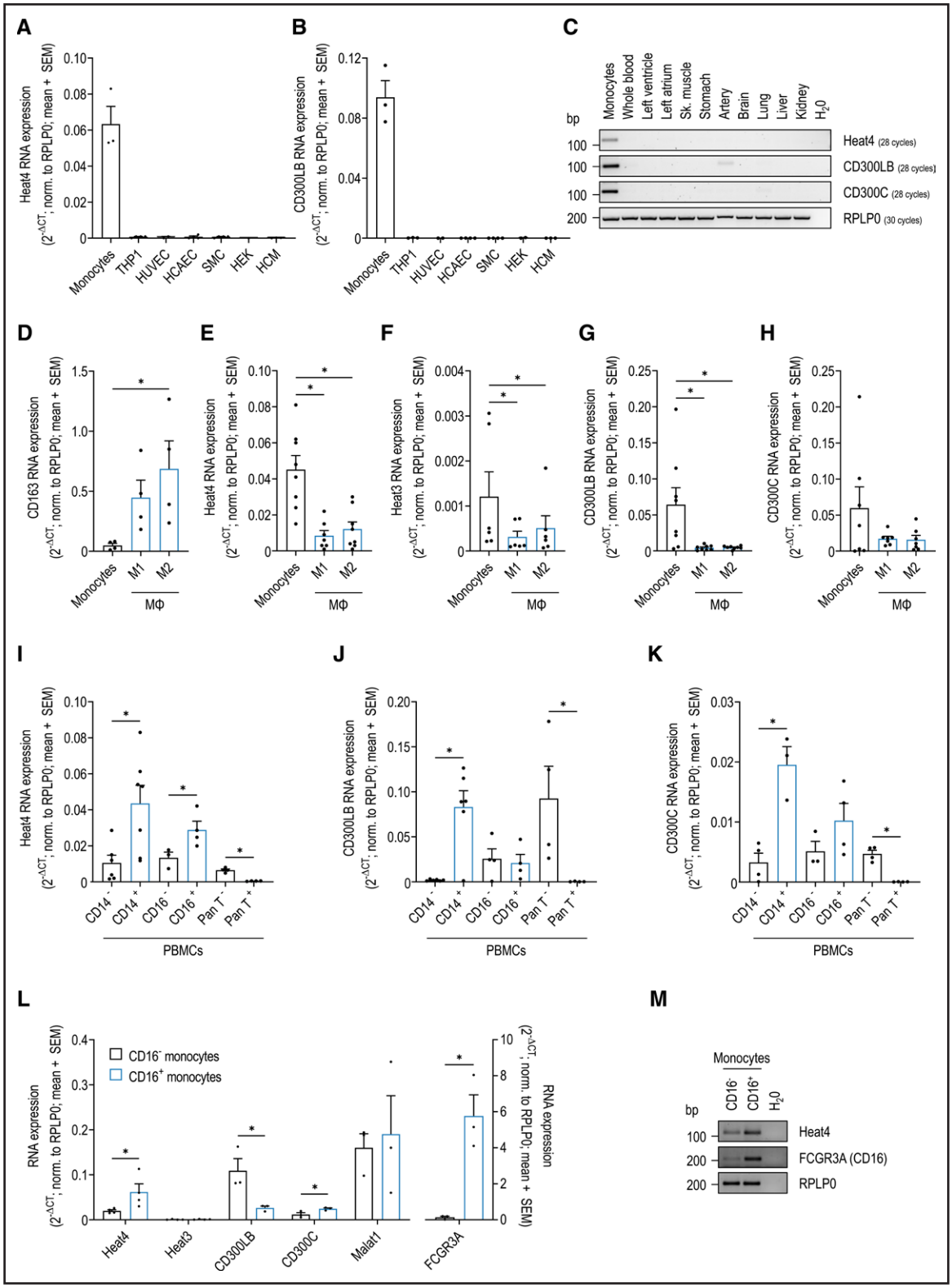

Figure 3. Differential expression of HEAT4 and other CD300 gene cluster members in monocyte subpopulations and their cellular origins.

RNA expression of *HEAT4* (heart failure–associated transcript 4 (**A**) and CD300LB (**B**) in human primary monocytes, the human monocytic cell line THP1, human umbilical vein endothelial cells (HUVECs), human coronary artery endothelial cells (HCAECs), smooth muscle cells (SMCs), human embryonic kidney cells (HEKs), and human cardiac myocytes (HCMs) measured by quantitative reverse transcription polymerase chain reaction (qRT-PCR; n=2–4). **C**, RNA expression of *HEAT4*, *CD300LB*, *CD300C*, and *RPLP0* in human blood derivatives (primary monocytes and whole blood) and tissues (left ventricle, left atrium, skeletal muscle, stomach, artery, brain, lung, liver, and kidney) visualized by (*Continued*)

Figure 3 Continued. agarose gel electrophoresis after qRT-PCR. A total of 28 PCR cycles were used for *HEAT4*, *CD300LB*, and *CD300C* and 30 for *RPLP0*. RNA expression of CD163 (n=4; repeated-measures [RM] 1-way ANOVA followed by Dunnett multiple comparisons test (**D**), *HEAT4* (n=7 or 8; mixed-model ANOVA followed by Dunnett multiple comparisons test; **E**), *HEAT3* (heart failure–associated transcript 3; n=6; Friedman test followed by Dunn multiple comparison test; **F**), *CD300LB* (n=8; RM 1-way ANOVA followed by Dunnett multiple comparisons test; **G**), and *CD300C* (n=7; RM 1-way ANOVA followed by Dunnett multiple comparisons test; **H**) in human primary monocytes and in M1 and M2 macrophages (MΦ) differentiated from monocytes using GM-CSF and M-CSF, respectively, measured by qRT-PCR. RNA expression of *HEAT4* (n=4–7; 2-tailed paired *t* tests; (**I**), *CD300LB* (n=4–7; 2-tailed paired *t* tests; (**J**), and *CD300C* (n=4; 2-tailed paired *t* tests; **K**) in human PBMCs separated into CD14 positive and negative, CD16 positive and negative, or Pan T positive and negative cells by magnetic activated cell sorting measured by qRT-PCR. **L**, RNA expression of *HEAT4*, *HEAT3*, *CD300LB*, *CD300C*, *MALAT1*, and *FCGR3A* (CD16) in human primary monocytes separated into CD16 positive and negative monocytes by magnetic activated cell sorting after isolation by counterflow centrifugal elutriation measured by qRT-PCR (n=4–5; 2-tailed paired *t* tests). **M**, Agarose gels showing the levels of *HEAT4*, *FCGR3A* (CD16), and *RPLP0* in representative fractions of CD16 positive and negative monocytes. Bar graphs are presented as mean+SEM. Statistical differences were calculated using paired *t* test or repeated measures or mixed-model 1-way ANOVA, both followed by Dunnett multiple comparisons test or Friedman test followed by Dunn multiple comparison test (*$P<0.05$).

respectively, indicating good differentiation between the HF and an age-matched control group, whereas *CD300LD* levels were unable to discriminate between these 2 groups (area under the receiver operating characteristic curve, 0.575; Figure 2A). To investigate the relationship between survival time of patients with HF and *HEAT3*, *HEAT4*, *CD300LB*, and *CD300LD* as continuous predictor variables, a Cox proportional hazards analysis was conducted. The analysis indicated an increased risk of all-cause mortality for patients with HF with higher levels for 3 of the predictor variables: *HEAT3*, *HEAT4*, and *CD300LD* (hazard ratio, 1.817 [P=0.008]; hazard ratio, 1.952 [P=0.009]; hazard ratio, 1.845 [P=0.004], respectively), with the exception of CD300LB (hazard ratio, 0.991 [P=0.980]; Figure 2B). The predictive property of *HEAT3*, *HEAT4*, and *CD300LD* was preserved after adjusting the models for age, sex, and high-sensitivity C-reactive protein (Table S4). Kaplan-Meier curves visualize the probability of survival in 2 groups of patients with HF with lower or higher RNA expression of *HEAT3*, *HEAT4*, *CD300LB*, and *CD300LD*, each divided by their median (Figure 2C through 2F). Individuals with *HEAT3*, *HEAT4*, and *CD300LD* values lower than the respective median had higher probability of survival as determined by the log-rank test. In summary, the levels of *HEAT3*, *HEAT4*, and *CD300LB* in whole blood show promise as potential biomarkers to distinguish patients with HF from people without HF. In addition, these lncRNAs, *HEAT3* and *HEAT4*, together with *CD300LD*, are predictive of all-cause mortality in patients with HF in the analyzed patient cohort over a follow-up of 7 years.

Differential Expression of *HEAT4* and *CD300* Gene Cluster Members in Monocyte Subpopulations and Their Cellular Origins

Characterizations of the expression of members of the *CD300* gene cluster in various human tissues and in different cell types within the human cardiovascular system revealed *HEAT4*, *CD300LB*, and *CD300C* to be selectively and highly expressed in monocytes (Figure 3A through 3C; Figure S2A and S2B). Expressions of *HEAT3*, *HEAT4*, *CD300LB*, and *CD300C* were not induced during monocyte differentiation into macrophage lineages, in contrast to the established macrophage marker CD163 (Figure 3D through 3H). Monocytes can be categorized into subpopulations depending on their expression of CD16. Analyzing *HEAT4* expression in different cell subsets separated from PBMCs indicated that *HEAT4* was predominantly present in CD14$^+$ and CD16$^+$ cells (Figure 3I). Among members of the *CD300* gene cluster, expressions of *CD300LB* and *CD300C* were enriched in CD14$^+$ cells and less in the T-cell fraction. (Figure 3J and 3K). Purification of monocytes using counter-flow centrifugal elutriation[41] followed by separation based on CD16 showed that *HEAT4*, *CD300C*, and CD16 (FCGR3A) were enriched in CD16$^+$ monocytes whereas *CD300LB* was not (Figure 3L and 3M). Because the expression level of *HEAT4* was unusually high for an lncRNA, similar to that of the protein-coding genes *CD300LB* and *CD300C*, we also compared the expression of the well-established lncRNA *MALAT1*, which is one of the most highly and ubiquitously expressed lncRNAs. *MALAT1* displayed higher expression than *HEAT4* and, like *HEAT3*, was only marginally enhanced in CD16$^+$ monocytes compared with CD16$^-$ monocytes (Figure 3L).

On the basis of all of these results, we decided to further characterize the role of *HEAT4* in HF.

HEAT4 Overexpression in Monocytes Promotes the CD16$^+$ Subpopulation and Suppresses the Inflammatory Response

We observed increased expression of *HEAT4* in HF patient samples using bulk RNA-seq, qPCR, and scRNA-seq in PBMCs of patients with HF (Figure 4A and 4B). Therefore, we aimed to examine the regulation of *HEAT4* expression in patients with HF. Our results from scRNA-seq revealed that *HEAT4* was expressed in CD16$^+$ monocytes of patients with HF and controls (Figure 4C through 4E). HF is associated with changed levels of inflammatory and anti-inflammatory cytokines,

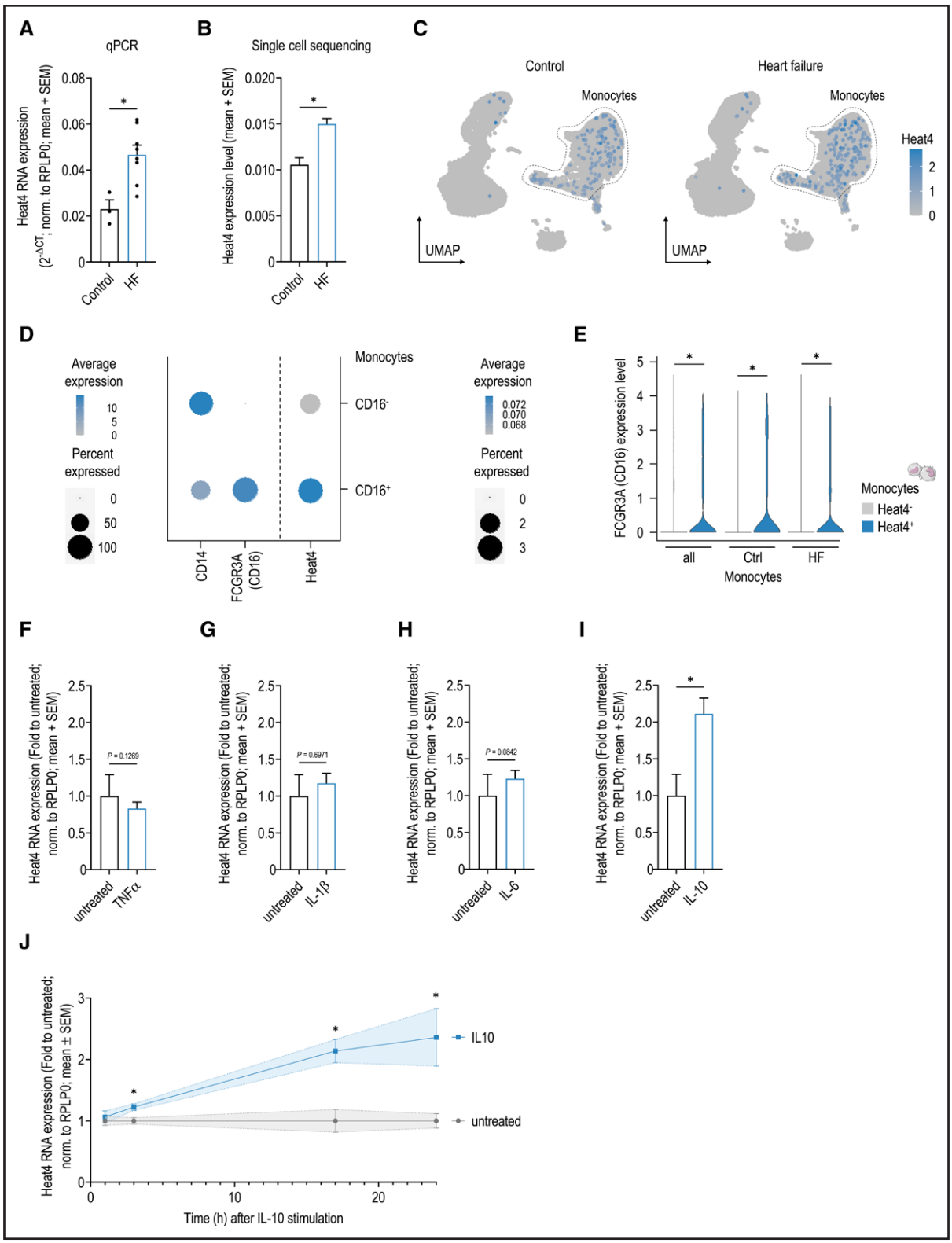

Figure 4. Regulation of HEAT4 expression.

Bar graphs showing RNA expression of *HEAT4* (heart failure–associated transcript 4) in peripheral blood mononuclear cells (PBMCs) of controls (n=3) and patients with heart failure (HF; n=8, cohort 1) measured by reverse transcription quantitative polymerase chain reaction (qPCR; 2-tailed unpaired *t* test; (**A**) and single-cell RNA sequencing (controls, n=24 573; HF, n=59 016; 2-tailed Mann-Whitney test; **B**). **C**, Feature plots showing *HEAT4* expression in 20 000 randomly selected cells of all individuals per condition. **D**, Dot plots show percentage of cells expressing *CD14*, *FCGR3A* (CD16), and *HEAT4* as well as their average expression level in monocyte subtypes (CD16⁻ and CD16⁺) of all samples together (controls+patients with HF; n=11). Left legend accounts for CD14 and FCGR3A (CD16) expression and right legend (*Continued*)

Figure 4 Continued. for *HEAT4* expression in CD16⁻ and CD16⁺ monocytes, respectively. **E**, Violin plots comparing the expression of *FCGR3A* (CD16) in *HEAT4* positive and negative monocytes from controls (n=3; 2-tailed Mann-Whitney test), patients with HF (n=8; 2-tailed Mann-Whitney test), and all samples together (controls+patients with HF, n=11; 2-tailed Mann-Whitney test). RNA expression of *HEAT4* in human primary monocytes after treatment with tumor necrosis factor α (TNFα; 10 ng/mL; **F**), interleukin (IL)−1β (10 ng/mL; (**G**), IL-6 (10 ng/mL; **H**), or IL-10 (100 ng/mL; **I**) for 24 hours relative to untreated (n=5; 2-tailed paired *t* tests). **J**, RNA expression of *HEAT4* in human primary monocytes after stimulation with IL-10 (100 ng/mL) for 1, 3, 17, and 24 hours (n=4; 2-tailed paired *t* tests). Bar graphs are presented as mean+SEM or mean±SEM (**G**, colored area). Statistical differences were calculated using paired and unpaired *t* test or Mann-Whitney test (*$P<0.05$). UMAP indicates uniform manifold approximation and projection.

such as tumor necrosis factor α (TNFα), IL-1β, IL-6, or IL-10. Treating monocytes with the anti-inflammatory cytokine IL-10 significantly increased *HEAT4* expression, whereas treating monocytes with inflammatory cytokines TNFα, IL-1β, or IL-6 had no effect on *HEAT4* expression (Figure 4F through 4I). Increased *HEAT4* expression in monocytes was already detectable 3 hours after stimulation with IL-10 (Figure 4J).

To investigate the function of increased *HEAT4* in monocytes, we induced the expression of *HEAT4* in human monocytes isolated by counterflow centrifugal elutriation with a purity of >90%. The overexpression of *HEAT4* led to reduced mRNA levels of inflammatory markers, including TNFα and members of the CCL chemokine family (*CCL2*, *CCL3*, *CCL4*, *CCL5*, and *CCL8*), in monocytes (Figure 5A through 5D; Figure S2C through S2E) and decreased protein levels of TNFα, IL-1β, and IL-6 in the supernatant (Figure 5F through 5H; Figure S2F through S2H). In contrast, genes with anti-inflammatory function and those involved in vascular healing, such as *CLEC10A* and *TGFBR2*, were induced (Figure 5C and 5E; Figure S2I). Most importantly, our data revealed that overexpression of *HEAT4* in monocytes also upregulated expression of the pan-monocyte marker CD14 and the monocyte subpopulation marker CD16, indicating an increase of CD16⁺ monocytes (Figure 5C and 5E). ScRNA-seq and flow cytometry analysis validated that overexpression of *HEAT4* led to an increased percentage of CD16⁺ monocytes and a decreased percentage of CD16⁻ monocytes, suggesting a monocyte subtype switch (Figure 5I through 5K; Figure S3A through S3L). In line with these results, the reduction of *HEAT4* increased the expression of inflammatory and M1 macrophage markers, such as TNFα, IL-6, CD86, IL-23, and IL-12, in monocytes treated with TNFα or lipopolysaccharides to induce an inflammatory response (Figure 5L through 5Q; Figure S4A). Taken together, these results demonstrate that *HEAT4* overexpression drives monocytes toward a CD16⁺ subpopulation and promotes anti-inflammatory functions.

Interaction of the lncRNA *HEAT4* With the Protein S100A9 in Monocytes

Next, we investigated how *HEAT4* in monocytes conferred the anti-inflammatory function. *HEAT4* has a poly-A tail and is located in the cytoplasm of monocytes (Figure 6A through 6C). The use of various analysis tools, such as the PhyloCSF score,[42] CPAT coding probability,[43] or ribosome profiling,[44] for predicting protein-coding potential or recognizing small open reading frames shows no potential for *HEAT4* to encode a protein or small peptide and also no translation initiation sites within the *HEAT4* transcript.[45] This is consistent with our results showing no protein formation upon in vitro translation (Figure 6D). To identify potential protein binding partners of *HEAT4* through antisense affinity selection, we first identified oligonucleotide-accessible regions within *HEAT4* by using RNase H-based cleavage of RNA–DNA heteroduplexes followed by reverse transcription qPCR (Figure 6E and 6F). We then designed a 2′O-Me-RNA antisense probe carrying a 3′-desthiobiotin-TEG group for streptavidin pulldown of *HEAT4*-protein complexes, using the accessible sequence of antisense oligonucleotide 6, and used this probe in monocyte cell lysates to enrich for *HEAT4* and its associated proteins (Figure 6G). The biotin-eluted protein fractions were separated by SDS-PAGE (Figure S5A and S5B) and analyzed by mass spectrometry,[46,47] and identified proteins were selected according to their average monocytic expression (Figure 6H through 6J; Figure S5C and S5D; Table S5). The analysis identified S100 calcium binding proteins A8 and A9 (S100A8 and S100A9), which have established functions in the inflammatory response of immune cells, among the top enriched proteins.[48,49] Antisense pulldown of *HEAT4* with subsequent immunoblot analysis validated the interaction of *HEAT4* lncRNA with both S100A8 and S100A9 protein (Figure 6K). However, RNA immunoprecipitation for S100A8 and additional RNA immunoprecipitation bulk RNA-seq for S100A9 only showed an interaction of *HEAT4* with S100A9 (Figure 6L through 6R; Figure S5E through S5H; Table S6). Because S100A8 and S100A9 frequently form heterodimers,[50] these results suggest that *HEAT4* binds S100A9 directly and binds S100A8 indirectly by means of its interaction with S100A9. To map the interaction site of *HEAT4* with the S100A9 protein, we designed *HEAT4* deletion constructs (*HEAT4*-Δ 1-10) using both the linear sequence and a possible secondary structure of *HEAT4* for the design, which we overexpressed in HEK-293 (human embryonic kidney) cells together with S100A9-Flag (Figure 6S and 6T; Figure S5I and S5J). RNA immunoprecipitation for *S100A9* revealed an interaction of full-length *HEAT4* with S100A9 in HEK-293

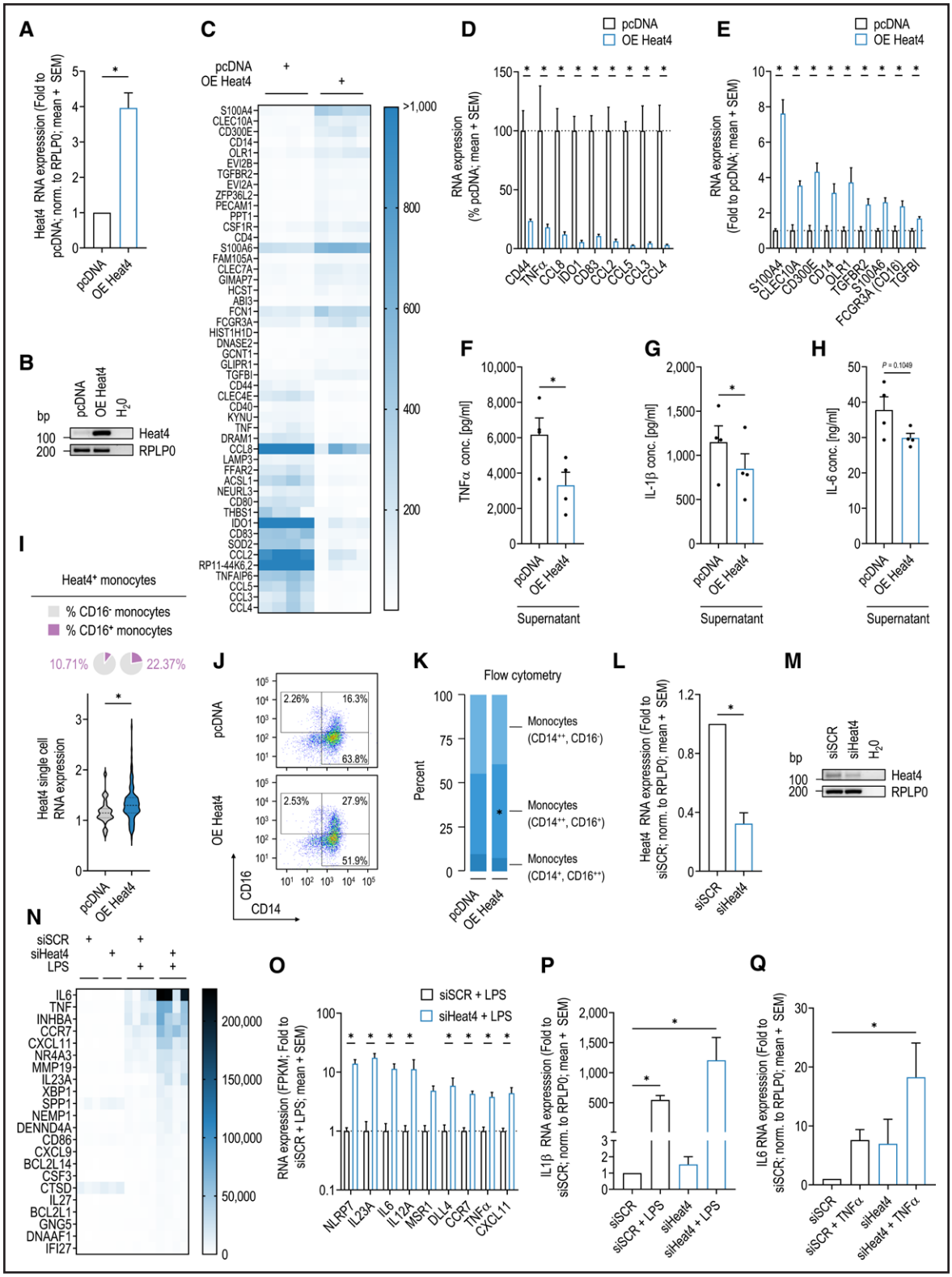

Figure 5. Overexpression of the lncRNA HEAT4 in human monocytes induces anti-inflammatory and vascular healing functions and promotes CD16+ monocyte populations.

Overexpression (OE) of *HEAT4* (heart failure–associated transcript 4) on RNA level measured by quantitative reverse transcription polymerase chain reaction (qRT-PCR; n=5; 2-tailed Wilcoxon matched-pairs signed rank test; **A**) and agarose gel electrophoresis; **B**). **C**, Heat map showing selection of the top upregulated and downregulated genes after *HEAT4* overexpression identified by next-generation bulk RNA sequencing (n=4). Validation of downregulated (n=4–6; 2-tailed paired *t* test; **D**) and upregulated (n=4; 2-tailed paired *t* test; **E**) genes in monocytes with *HEAT4* OE by qRT-PCR. Protein levels of tumor necrosis factor α (TNFα; n=4; 2-tailed paired *t* test; **F**), interleukin (IL)−1β (n=4; (*Continued*)

Figure 5 Continued. 2-tailed paired *t* test; **G**), and IL-6 (n=4; 2-tailed paired *t* test; **H**) in supernatants of human primary monocytes without and with HEAT4 OE measured by ELISA. **I**, Single-cell RNA sequencing of human primary monocytes without or with *HEAT4* OE was performed. Monocytes in both conditions were divided into HEAT4$^+$ and HEAT4$^-$ monocytes on the basis of the *HEAT4* expression of each individual cell. Percentage of CD16$^+$ monocytes among the HEAT4$^+$ monocytes is given in the upper panel; the left pie chart shows control condition (pcDNA) and right pie chart shows OE *HEAT4*. *HEAT4* expression level of HEAT4$^+$ monocytes for both conditions is given in the bottom panel (pcDNA, n=28; OE *HEAT4*, n=152; 2-tailed Mann-Whitney test). **J**, Representative flow cytometric measurements of human primary monocytes without or with *HEAT4* overexpression labelled with antibodies targeting CD14 and CD16. **K**, Stacked bar plots showing percentages of the 3 monocyte subtypes (CD14^{++}, CD16$^-$), (CD14^{++}, CD16$^+$), and (CD14$^+$, CD16^{++}) among human primary monocytes without or with *HEAT4* overexpression on the basis of flow cytometry analysis (n=5; 2-tailed paired *t* test). Knockdown of *HEAT4* was validated on RNA level by qRT-PCR (n=5; 2-tailed paired *t* test; **L**) and agarose gel electrophoresis (**M**). **N**, Heat map showing genes with altered expressions in monocytes without and with *HEAT4* knockdown and in the presence and absence of lipopolysaccharides (100 ng/mL, 6 hours) analyzed by next-generation bulk RNA sequencing (n=4). **O**, Top upregulated genes in monocytes with *HEAT4* knockdown and lipopolysaccharides (100 ng/mL, 6 hours) treatment (FPKM, n=4; 2-tailed paired *t* tests). RNA expression of IL-1β (n=5; ordinary 2-way ANOVA followed by Tukey multiple comparisons test; **P**) and IL-6 (n=7; ordinary 2-way ANOVA followed by Tukey multiple comparisons test; **Q**) in human primary monocytes after *HEAT4* knockdown and lipopolysaccharides (100 ng/mL, 6 hours) or TNFα (10 ng/mL, 6 hours) treatment measured by qRT-PCR. Bar graphs are presented as mean+SEM. Statistical differences were calculated using paired and unpaired *t* test or Wilcoxon matched-pairs signed rank test or Mann-Whitney test or ordinary 2-way ANOVA followed by Tukey multiple comparisons test (*P<0.05).

cells, confirming our results from monocytes (Figure 6U). Among the deletion constructs, the region at the end of exon 1 at the transition to exon 2 of *HEAT4* appears to be most important for the interaction with *S100A9* (*HEAT4*-Δ3, -Δ7, -Δ9), but other elements also appear to mediate the interaction, such as a possible secondary structure at the 3′-end and 5′-beginning of the *HEAT4* transcript (see *HEAT4*-Δ6 and -Δ10), although to a lesser extent.

HEAT4 Reduces Extracellular S100A8/A9 Levels and Leads to Nuclear Translocation of S100A9

Reducing S100A9 levels in monocytes decreased TNFα-induced inflammation, as shown by the reduced induction of IL-6 expression, whereas *HEAT4* expression was not affected (Figure S6A through S6C). Conversely, overexpression of S100A9 increased the expression of IL-6, which was countered by co-overexpression of *HEAT4* (Figure 7A through 7C). Overexpression of *HEAT4* had no effect on the mRNA or protein level of S100A9 or the S100A8 mRNA level in monocytes (Figure 7D and 7E; Figure S6D through S6G). After *HEAT4* overexpression, we observed a decreased release of the S100A8/A9 heterodimer from monocytes (Figure 7F and 7G). These results suggest that *HEAT4* interacts with S100A9 in monocytes and suppresses the inflammatory response by inhibiting the release of the S100A8/A9 heterodimer. *HEAT4* overexpression or IL-10 treatment resulted in translocation of S100A9 into the nucleus (Figure 7H through 7J; Figure S6H). The chromatin profile of S100A9 in monocytes and the overlap of the interaction peaks corresponded to active enhancer and promoter elements (Figure 7K through 7N). We identified a top interaction motif for S100A9 within the significant peaks by a de novo search for motif enrichments (Figure 7O; Figure S6I through S6K). Chromatin immunoprecipitation sequencing[51] of S100A9 after *HEAT4* overexpression and IL-10 treatment shows increased binding of S100A9 to promoter and enhancer elements of genes with increased expression after *HEAT4* overexpression (Figure 7P; *HEAT4* overexpression: Figure 5C). We showed that *HEAT4* reduces the extracellular release of S100A9, but also leads to translocation of S100A9 to the nucleus, where it interacts with active promoters and enhancers.

HEAT4 Overexpression in Monocytes Enhances Endothelial Barrier Regeneration and Promotes Vascular Healing

CD16$^+$ monocytes are associated with ischemic diseases, in which they maintain vascular homeostasis by patrolling the endothelium, in search of injury.[19,20,52] To investigate the potential effect of *HEAT4* on vascular homeostasis after injury, we first analyzed the regulation of *HEAT4* in ischemic heart diseases and then evaluated the effect of *HEAT4*-overexpressing monocytes on endothelial barrier function in an inflammatory setting. *HEAT4* levels were increased in patients after acute MI (cohort 4; n=42), both ST-segment–elevation MI (n=21) and non–ST-segment–elevation MI (n=21), as well as in patients after cardiogenic shock (cohort 5; n=4), compared with controls (Figure 8A through 8D; Table S7 and S8). Our results show that human monocytes overexpressing *HEAT4* provide better regeneration of endothelial barrier function after an inflammatory stimulation (Figure 8E and 8F). The lncRNA *HEAT4* does not exist in mice. Neither the sequence nor the genomic locus shows evolutionary conservation. Therefore, a humanized mouse model of vascular injury was used to investigate the in vivo function of *HEAT4*. We injured the left carotid artery[53] of nonobese diabetic–severe combined immunodeficiency mice and injected human monocytes without or with *HEAT4* overexpression (Figure 8G and 8H). We excised the left carotid arteries 3 days later, quantified the re-endothelialized area, and found that carotid arteries of nonobese diabetic–severe combined immunodeficiency mice injected with human monocytes

ORIGINAL RESEARCH ARTICLE

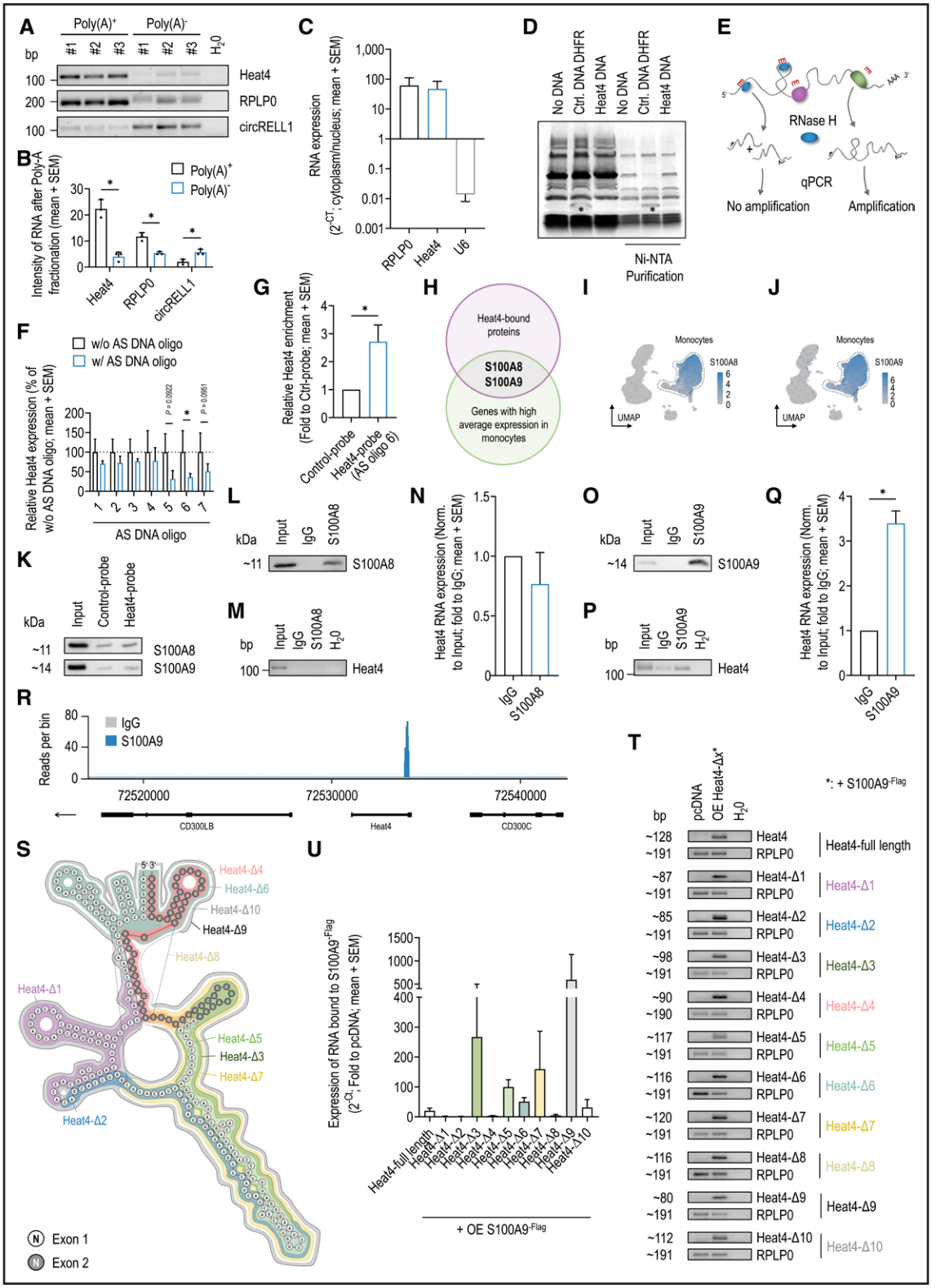

Figure 6. Interaction of the lncRNA HEAT4 with S100A9 in the cytoplasm of human monocytes.

A, Representative image and quantification (**B**) of *HEAT4* (heart failure–associated transcript 4), *RPLP0* (poly[A] positive control), and circ*RELL1* (poly[A] negative control) RNAs in poly(A) positive and negative RNA fractions of human primary monocytes separated by oligo d(T)$_{25}$ magnetic beads and analyzed by agarose gel electrophoresis (n=3; 1-tailed [positive controls: poly(A) positive: RPLP0; poly(A) negative: circRELL1] and 2-tailed [HEAT4] paired *t* tests). **C**, Localizations of *HEAT4*, *RPLP0* (cytoplasmic control), and U6 (nuclear control) RNAs in nuclear and cytoplasmic fractions of human primary monocytes analyzed by quantitative reverse transcription polymerase chain reaction (qRT-PCR). **D**, In vitro translations of *HEAT4* and *DHFR* (positive control) without and with Ni-NTA purification analyzed by SDS-PAGE using a (*Continued*)

Figure 6 Continued. 4% to 20% gel followed by Coomassie staining. Asterisks indicate the translated DHFR (dihydrofolate reductase) protein. **E**, Schematic illustration of the RNA accessibility assay to identify probe-accessible sites on the *HEAT4* RNA. RNase H (blue) can recognize and cleave the RNA in antisense DNA oligonucleotide (red)–RNA (gray) heteroduplexes. Inaccessible sites (green and purple; eg, due to binding of proteins) are not cleaved and result in similar *HEAT4* RNA expression as when no antisense DNA oligonucleotide was added. **F**, Accessible regions of the *HEAT4* RNA indicated by reduced *HEAT4* expression signal using monocyte lysates treated with or without an antisense DNA oligonucleotide (AS DNA oligo) followed by RNase H digestion and analyzed by qRT-PCR (n=3–5; 1-tailed paired *t* test and Wilcoxon matched-pairs signed rank test). **G**, *HEAT4* enrichment after RNA affinity purification using against-*HEAT4* directed 2′O-Me-RNA oligonucleotides (sequence of AS oligo 6) in lysates of human primary monocyte analyzed by qRT-PCR (n=3 per elution; 2-tailed Wilcoxon matched-pairs signed rank test). **H**, Venn diagram showing overlaps between proteins bound to *HEAT4* isolated by *HEAT4* RNA affinity purification and identified by mass spectrometry with genes enriched in monocytes detected by single-cell RNA sequencing. Feature plots showing S100A8 (**I**) and S100A9 (**J**) expression in 20 000 peripheral blood mononuclear cells of controls of cohort 1 (n=3). **K**, RNA affinity purification of *HEAT4* using 2′O-Me-RNA oligonucleotides with subsequent immunoblotting for S100A8 and S100A9. RNA immunoprecipitation (RIP) of S100A8 in human primary monocytes after *HEAT4* overexpression (OE) with subsequent immunoblotting for S100A8 (**L**) and detection of *HEAT4* (**M**) by agarose gel electrophoresis after qRT-PCR. **N**, Quantitation of *HEAT4* bound to S100A8 isolated by RIP and analyzed by qRT-PCR (n=4; 1-tailed paired *t* test). RIP of S100A9 in human primary monocytes after *HEAT4* OE with subsequent immunoblotting for S100A9 (**O**) and detection of *HEAT4* (**P**) by agarose gel electrophoresis after qRT-PCR. **Q**, Quantitation of *HEAT4* bound to S100A9 isolated by RIP and analyzed by qRT-PCR (n=3; 1-tailed paired *t* test). **R**, Reads per bin of *CD300LB*, *HEAT4*, and *CD300C* (all hg19) detected by next-generation bulk RNA sequencing in monocytes after RIP using immunoglobulin G (IgG) or S100A9 antibody. All genes are located on the reverse strand (arrow pointing left, ←). **S**, Schematic illustration of the distribution of the 10 *HEAT4* deletion constructs Δ 1 to Δ 10 on *HEAT4* folded according to the prediction of RNAfold WebServer. Exons 1 and 2 of *HEAT4* are distinguished on the basis of their color. **T**, Agarose gels showing the levels of *HEAT4*, *RPLP0*, and the *HEAT4* deletion constructs Δ 1 through Δ 10 in human embryonic kidney (HEK) cells after cotransfection of S100A9$^{\text{-Flag}}$ and the respective deletion construct or *HEAT4*–full length. **U**, RNA expression of *HEAT4*–full length and *HEAT4* deletion constructs Δ 1 through Δ 10 in HEK cells after cotransfection of S100A9$^{\text{-Flag}}$ and *HEAT4*–full length or *HEAT4* deletion constructs Δ 1 through Δ 10 and subsequent Flag-IP compared with Flag-IP of pcDNA-transfected HEK cells (n=2–5). Bar graphs show mean+SEM. Statistical differences were calculated using paired and unpaired *t* test or Wilcoxon matched-pairs signed rank test or Mann-Whitney test (*P<0.05). UMAP indicates uniform manifold approximation and projection.

overexpressing *HEAT4* regenerated faster than those injected with control monocytes (Figure 8I and 8J). These results suggest that human monocytes overexpressing *HEAT4* can improve the regeneration of endothelial barrier function in an inflammatory setting and enhance the re-endothelialized area of carotid arteries in a humanized mouse model of vascular injury.

DISCUSSION

This study uncovers the lncRNA *HEAT4* as a regulator of monocyte subtypes toward an anti-inflammatory phenotype. This research shows for the first time that specific lncRNAs modulate monocyte function, dampen inflammation, and promote the restoration of endothelial barrier function and vascular injury. The identification of the ability of *HEAT4* to suppress the release of the S100A8/A9 heterodimer and promote the translocation of S100A9 into the nucleus, where it binds to active promoter and enhancer elements, reveals a novel function for lncRNAs and advances our understanding of their versatile regulatory roles in immune responses. These findings may lead to the development of targeted interventions aimed at harnessing immune responses and fostering vascular recovery across various inflammatory conditions, including CVDs.

The results demonstrate that *HEAT4* is enriched in CD16$^+$ monocytes of patients with HF, suggesting the potential involvement of *HEAT4* in the immune regulation of monocytes in HF. CD16$^+$ monocytes are known for their active patrolling of the vascular endothelium to eliminate damaged cells and debris, and have been implicated in various human diseases, including CVDs, cancer, and autoimmune disorders.[7,20] CD16$^+$ monocytes possess unique phenotypic and functional traits that distinguish them from other monocyte subsets, such as their adhesion to the endothelial wall and their association with wound-healing processes,[52] and their dysregulation can affect disease progression considerably.[54]

CD16$^+$ monocytes have been reported to exhibit profibrotic phenotypes in chronic conditions.[55–57] CD16$^+$ cells play a role in wound and vascular healing. We observed an increase in the TGFβ signaling pathway in monocytes after *HEAT4* overexpression. This relationship may explain the observed association between higher *HEAT4* levels and poorer survival in patients with HF. The observation that overexpression of *HEAT4* enhances the regeneration of endothelial barrier function suggests its potential involvement in promoting the perivascular functions of CD16$^+$ monocytes.[58] By modulating the inflammatory response and promoting vascular healing, CD16$^+$ monocytes, in conjunction with *HEAT4*, may contribute to the resolution of inflammation and the restoration of vascular homeostasis in human diseases.

The observation that *HEAT4* is induced by the anti-inflammatory cytokine IL-10 and appears to be an anti-inflammatory mediator itself is interesting given its association with unfavorable cardiovascular outcomes. The inflammatory process has pro- and anti-inflammatory phases, and prolonged activation of both pro- and anti-inflammatory processes is associated with unfavorable effects (eg, in chronic HF or cardiac fibrosis).[13–15] Also, IL-10 is elevated in accelerated atherosclerosis after deep vein thrombosis, whereby deep vein thrombosis and natural thrombus dissolution are processes that are

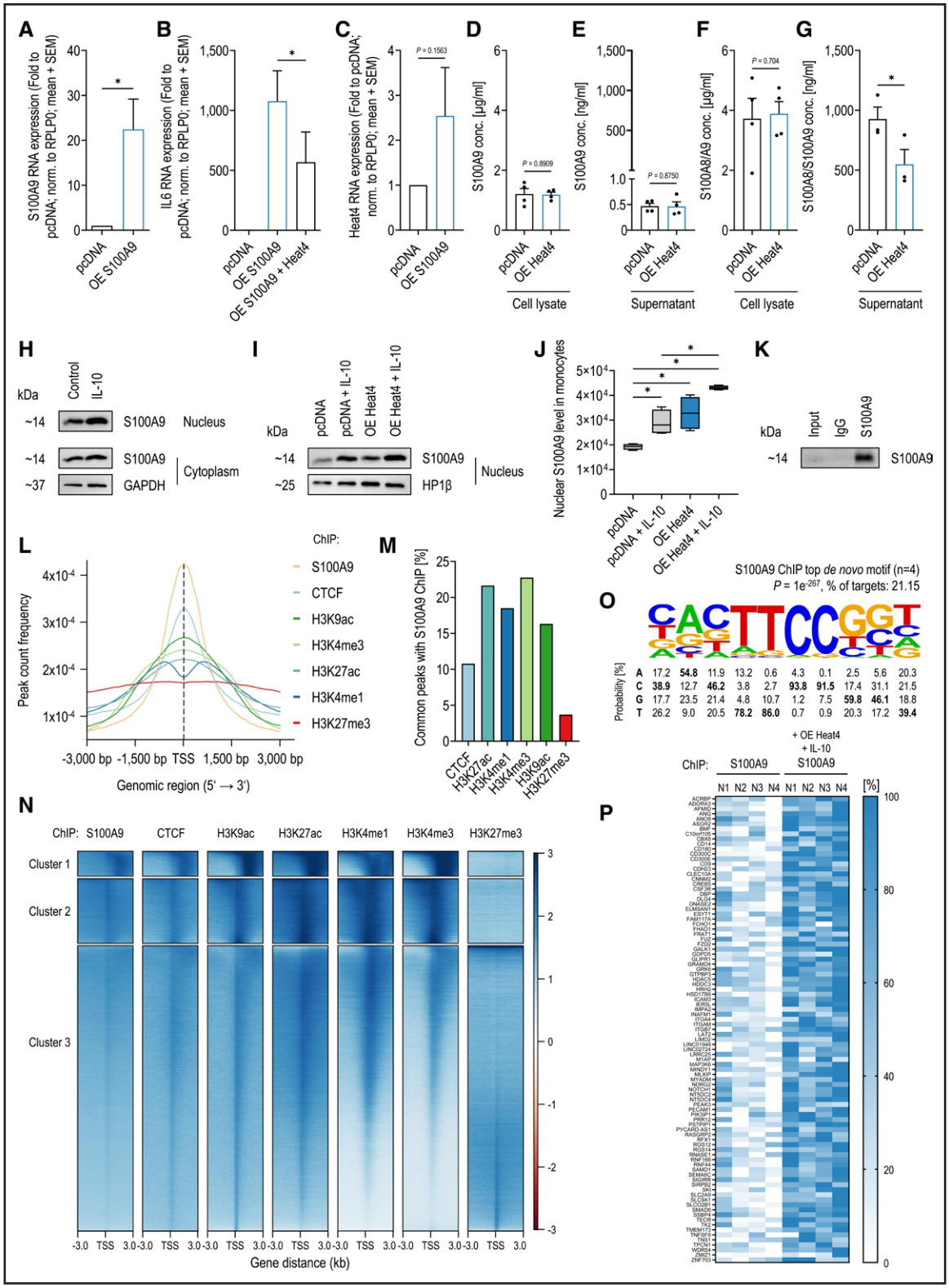

Figure 7. HEAT4 reduces extracellular S100A8/A9 levels and leads to nuclear translocation of S100A9.
A, RNA level of *S100A9* in monocytes without or with *S100A9* overexpression (OE; n=7; 2-tailed Wilcoxon matched-pairs signed rank test). **B**, Interleukin (IL)–6 RNA expression in monocytes without or with *S100A9* OE alone or with co-overexpression of *HEAT4* (heart failure–associated transcript 4) measured by quantitative reverse transcription polymerase chain reaction (n=5; 1-tailed Wilcoxon matched-pairs signed rank test). **C**, *HEAT4* RNA expression in monocytes without or with *S100A9* OE (n=6; 2-tailed Wilcoxon matched-pairs signed rank test). S100A9 protein levels in cell lysates (n=4; 2-tailed paired *t* test; **D**) and supernatants (n=4; 2-tailed Wilcoxon matched-pairs signed rank test; **E**) of monocytes without or with *HEAT4* overexpression measured by ELISA. S100A8/A9 heterodimer protein levels in cell lysates (n=4; 2-tailed (*Continued*)

Figure 7 Continued. paired *t* test; **F**) and supernatants (n=3; 2-tailed paired *t* test; **G**) of monocytes without or with *HEAT4* overexpression measured by ELISA. **H**, Nuclear and cytoplasmic S100A9 levels after treatment of human primary monocytes with IL-10 (100 ng/mL, 24 hours; control: pcDNA) identified by nucleus-cytoplasm fractionation followed by immunoblotting for S100A9 and GAPDH (cytoplasmic marker). Cytoplasmic samples were diluted 1:20 before loading. **I**, Nuclear S100A9 levels after *HEAT4* OE and IL-10 treatment (100 ng/mL, 24 hours) identified by nucleus-cytoplasm fractionation followed by immunoblotting for S100A9. Exemplary blot showing HP1β (nucleus marker). Densitometric analysis of *S100A9* (**I**, **top**) is shown (n=4; ordinary 2-way ANOVA followed by Tukey multiple comparisons test; **J**). **K**, Chromatin immunoprecipitation (ChIP) of S100A9 with subsequent immunoblotting for S100A9. **L**, Average profile of S100A9 (n=4) and histone modification ChIP peaks (obtained from USCS) binding to transcription start site (TSS) region. **M**, Percentage of peak overlap of S100A9 ChIP (n=4) and histone modification peaks. **N**, Heat map of S100A9 (n=4) and chromatin occupancy of the indicated factors at ±3000 bp of TSS. **O**, Top de novo DNA motif identified after S100A9 ChIP (n=4). **P**, Heat map of differential peaks (found in each of the 8 samples) enriched in S100A9 ChIP after IL-10 treatment and *HEAT4* OE compared with *S100A9* ChIP without treatment. Selected genes are shown that were increased after *HEAT4* OE (Figure 5C). Statistical differences were calculated using paired *t* test or Wilcoxon matched-pairs signed rank test or ordinary 2-way ANOVA followed by Tukey multiple comparisons test (*$P<0.05$).

closely associated with (vascular) wound healing.[59,60] This suggests that the anti-inflammatory and healing function of *HEAT4* is beneficial after acute inflammatory stimuli or injury, but produces adverse effects upon long-term activation, similar to other anti-inflammatory molecules, such as TGF-β.

Our results show that upregulation of *HEAT4* in immune cells is associated with an increased proportion of CD16$^+$ monocytes, whereas decreased expression of *HEAT4* is linked to an enhanced polarization of monocytes toward M1 macrophages. These findings demonstrate the role of *HEAT4* in modulating monocyte fate and function and suggest its relevance in promoting monocytes toward a CD16$^+$ phenotype, which has been observed in several human diseases.[58] The results of our study show that *HEAT4* is a key regulator in driving the balance between CD16$^+$ monocytes and M1 macrophages, beyond classical cytokine signaling.

The interaction between *HEAT4* and S100A8/A9 proteins provides mechanistic insights into the anti-inflammatory properties of *HEAT4*. The interaction with S100A9 is mainly mediated by the region at the end of exon 1 at the transition to exon 2 of *HEAT4*, but nonlinear RNA elements also appear to mediate the interaction, such as a possible secondary structure at the 3′-end and 5′-end of the *HEAT4* transcript, albeit to a lesser extent. Because S100A9 does not possess a classic nucleic acid binding domain, it is likely that the interaction of S100A9 with *HEAT4* is mediated in part by secondary RNA structures of *HEAT4*. *HEAT4* overexpression results in decreased release of the S100A8/A9 heterodimer, thereby suppressing IL-6–induced inflammation. The alarmins S100A8/A9 are increasingly released by immune cells such as neutrophils and monocytes after inflammatory stimuli.[61,62] Extracellular concentrations of S100A8/A9 amplify the inflammatory response by inducing immune cells such as neutrophils and macrophages to release more cytokines, thereby initiating a cycle and amplifying the inflammatory response.[63–65] Although monocytes are found in comparatively lower numbers than neutrophils, the S100A8/A9 released by monocytes can activate other immune cells, such as neutrophils and macrophages, as an inflammatory trigger. Extracellular S100A8/A9 can activate neutrophils in a dose-dependent manner.[65] It is conceivable that the release of S100A8/A9 controlled by *HEAT4* regulates interactions between different immune cell types. For example, there is evidence that S100A8/A9 released by neutrophils during ST-segment–elevation MI can be taken up by platelets.[66] Our data indicate that *HEAT4* inhibits the extracellular release of S100A8/A9 from monocytes and thus may play a limiting role in the self-amplifying, immune cell–spanning inflammatory signaling of monocytes to activate neutrophils with S100A8/A9 in the center. Moreover, S100A9 was shown to be an important regulator of the conversion of inflammatory monocytes to reparatory immune cells in mice after acute MI.[67] The ability of *HEAT4* to suppress the release of the S100A8/A9 heterodimer, an inflammatory alarmin produced by activated immune cells, introduces a new dimension to the regulatory mechanisms of immune cell function and inflammation. Under physiologic conditions, S100A8 and S100A9 are among the most highly expressed mRNAs in immune cells such as neutrophils and monocytes, where they have important functions in the regulation of inflammation.[68] We show a translocation of S100A9 into the nucleus of monocytes, both after *HEAT4* overexpression and after treatment with IL-10, consistent with data showing nuclear translocation of S100A9 in breast cancer cells.[69] The binding of S100A9 to active promoter and enhancer elements of *HEAT4*-regulated genes that we observed is enhanced by *HEAT4* overexpression and treatment with IL-10. Thus, we show that in addition to its well-described pro-inflammatory functions, S100A9 may also have anti-inflammatory effects at the chromatin level of monocytes. The regulated genes, such as the CD16$^+$ monocyte marker *CLEC10A*,[70] but also CD11b (*ITGAM* [integrin alpha M]), which regulates vascular patrolling and crawling of CD16$^+$ monocytes,[52] show a strong association with anti-inflammatory CD16$^+$ monocyte function.

This novel function of *HEAT4* as an inhibitor of protein release represents an important and previously unexplored role for lncRNAs,[71] expanding our understanding of the effect of circulating noncoding RNAs on immune regulation.

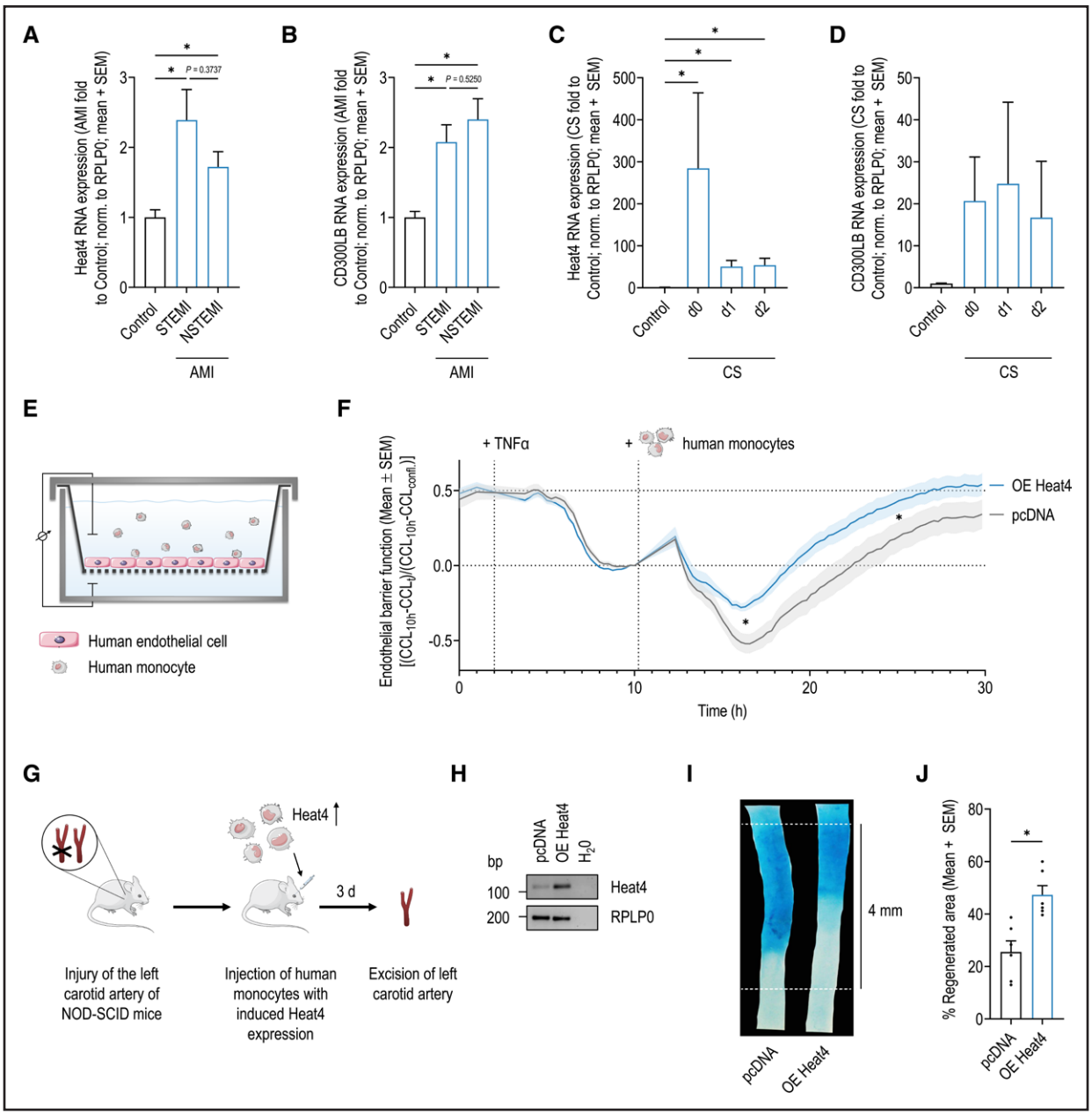

Figure 8. HEAT4 overexpression in monocytes enhances the endothelial barrier regeneration and promotes vascular healing. **A**, RNA levels of *HEAT4* (heart failure–associated transcript 4) determined by quantitative reverse transcription polymerase chain reaction (qRT-PCR) in peripheral blood mononuclear cells (PBMCs) from patients with acute myocardial infarction (AMI) separated into (STEMI; n=21) and (NSTEMI; n=21) relative to controls (n=23; cohort 4; Kruskal-Wallis followed by Benjamini-Krieger-Yekutieli test). **B**, RNA levels of CD300LB determined by qRT-PCR in PBMCs of patients with AMI separated into STEMI (n=19) and NSTEMI (n=21) relative to controls (n=23; cohort 4; Kruskal-Wallis followed by Benjamini-Krieger-Yekutieli test). **C**, RNA levels of *HEAT4* determined by qRT-PCR in whole blood of patients with cardiogenic shock (CS; n=4) relative to controls (n=5; cohort 5; Kruskal-Wallis followed by Benjamini-Krieger-Yekutieli test). d0 represents day of revascularization; d1, 1 day after revascularization; and d2, 2 days after revascularization. **D**, RNA levels of CD300LB determined by qRT-PCR in whole blood of patients with CS (n=4) relative to controls (n=4; cohort 5; Kruskal-Wallis followed by Benjamini-Krieger-Yekutieli test). d0 represents day of revascularization; d1, 1 day after revascularization; and d2, 2 days after revascularization. **E**, Schematic illustration of the experimental setup for measuring the endothelial barrier function. **F**, The endothelial barrier function of human endothelial cells treated with 10 ng/mL tumor necrosis factor α (TNFα) followed by incubation with human primary monocytes without or with *HEAT4* overexpression (OE; n=3; 2-tailed paired *t* tests). Test time points were selected a priori, covering maximal EC permeability and recovering phase after TNFα treatment. **G**, Schematic illustration of the experimental setup of a carotid artery injury model using nonobese diabetic–severe combined immunodeficiency (NOD-SCID) mice injected with human primary monocytes. The left carotid artery was excised after 3 days and examined. **H**, Expression of *HEAT4* in human monocytes without or with *HEAT4* OE used in the carotid artery injury model detected using agarose gel electrophoresis. Light microscopy image (**I**) and quantification (**J**) of reendothelialized areas at day 3 after carotid injury in NOD-SCID mice in *HEAT4* OE (n=6) and control (n=6; 2-tailed unpaired *t* test) groups. Graphs are presented as mean+SEM. Statistical differences were calculated using paired and unpaired *t* test or Kruskal-Wallis followed by Benjamini-Krieger-Yekutieli test (*$P<0.05$).

We also investigated the effect of *HEAT4* on vascular homeostasis and revealed the ability of *HEAT4* to enhance the regeneration of the endothelial barrier function in the context of inflammation. Injecting human monocytes overexpressing *HEAT4* into a humanized mouse model of vascular injury resulted in accelerated reendothelialization of injured carotid arteries. These findings underscore the therapeutic potential of *HEAT4* in promoting vascular repair processes and maintaining vascular integrity, especially in the context of HF.[72] *HEAT4* is a primate-specific lncRNA, which emphasizes the importance of studying human-specific molecular mechanisms in immune-mediated diseases, particularly in HF.[72]

The findings of this study underscore the crucial role of *HEAT4* in immune cell modulation, inflammation suppression, and maintenance of vascular homeostasis, particularly in the context of HF. The identification of *HEAT4* as a key regulator of monocyte function highlights its potential therapeutic implications, opening up avenues for the development of targeted interventions to address immune dysregulation and vascular dysfunction in patients with HF. Moreover, given the broader involvement of monocytes and inflammation in various human diseases, the functional importance of *HEAT4* may extend beyond HF, making it a potential target for therapeutic strategies aimed at mitigating immune dysregulation and vascular complications in a broader range of conditions. Future research should delve deeper into the precise molecular mechanisms underlying the effects of *HEAT4* and its clinical relevance to fully exploit its therapeutic potential in HF and other immune-related disorders.

The study establishes an association among lncRNAs, CD16$^+$ monocytes, and CVDs. Targeting lncRNAs may represent an innovative approach to control monocyte-mediated inflammation in CVDs.

ARTICLE INFORMATION

Received February 21, 2024; accepted June 11, 2024.

Affiliations

Klinik und Poliklinik für Kardiologie, Universitätsklinikum Leipzig, Germany (J.M.K., I.A.G., M.W., S.E., T.M., M.N.M.-W., A.K., K.E.K., V.F., S.G., U.L., J.-N.B.). Central German Heart Alliance (J.M.K., I.A.G., M.W., S.E., T.M., M.N.M.-W., A.K., K.E.K., V.F., S.G., H.T., U.L., J.-N.B.). Institute of Clinical Immunology, University of Leipzig, Germany (R.W.). Department of Cardiology and Pneumology, University Medical Center of Göttingen, Germany (T.G.-V., S.v.H.). German Center for Cardiovascular Research (DZHK), Partner Site Göttingen, Germany (T.G.-V., S.v.H.). Helmholtz Institute for Metabolic, Obesity and Vascular Research (HI-MAG) of the Helmholtz Zentrum München at the University of Leipzig and University Hospital Leipzig, Germany (B.N.S.). German Research Center for Environmental Health, GmbH, Metabolomics and Proteomics Core, Helmholtz Zentrum München, Germany (A.-C.K.). Department of Cardiology, Heart Center at University of Leipzig, Germany (K.-P.K., S.R., H.T., P.L.). Department of Cardiology, Universitätsmedizin Johannes Gutenberg-University, Mainz, Germany (K.-P.K., S.R., P.L.). Medizinische Klinik 4: Nephrologie, Universitätsklinikum Frankfurt, Frankfurt am Main, Germany (T.S.). Else Kroener-Fresenius Center for Nephrological Research, Goethe University, Frankfurt, Germany (T.S.).

Acknowledgments

The authors thank Tino Röxe, Anne Marie Müller, and Ellen Becker for technical support.

Sources of Funding

This work was funded by the German Research Foundation (Deutsche Forschungsgemeinschaft), project numbers BO 5271/5-1 to Dr Boeckel and GA 3049/3-1 to Dr Gaul, and through SFB 1052, project number 209933838, subproject C06, to Drs Boeckel and Laufs. Dr Speer is supported by the Else Kroener-Fresenius Foundation and Deutsche Forschungsgemeinschaft (SFB TRR 219, project number 322900939).

Disclosures

None.

Supplemental Material

Methods
Tables S1–S16
Excel Files S1–S8
Figures S1–S8
Video S1
Uncropped gel blots

REFERENCES

1. Greten FR, Eckmann L, Greten TF, Park JM, Li Z-W, Egan LJ, Kagnoff MF, Karin M. IKKβ links inflammation and tumorigenesis in a mouse model of colitis-associated cancer. *Cell*. 2004;118:285–296. doi: 10.1016/j.cell.2004.07.013
2. Pikarsky E, Porat RM, Stein I, Abramovitch R, Amit S, Kasem S, Gutkovich-Pyest E, Urieli-Shoval S, Galun E, Ben-Neriah Y. NF-κB functions as a tumour promoter in inflammation-associated cancer. *Nature*. 2004;431:461–466. doi: 10.1038/nature02924
3. McInnes IB, Schett G. Cytokines in the pathogenesis of rheumatoid arthritis. *Nat Rev Immunol*. 2007;7:429–442. doi: 10.1038/nri2094
4. Huseby ES, Liggitt D, Brabb T, Schnabel B, Öhlén C, Goverman J. A pathogenic role for myelin-specific CD8+ T cells in a model for multiple sclerosis. *J Exp Med*. 2001;194:669–676. doi: 10.1084/jem.194.5.669
5. Levine B, Kalman J, Mayer L, Fillit HM, Packer M. Elevated circulating levels of tumor necrosis factor in severe chronic heart failure. *N Engl J Med*. 1990;323:236–241. doi: 10.1056/NEJM199007263230405
6. Everett BM, Cornel JH, Lainscak M, Anker SD, Abbate A, Thuren T, Libby P, Glynn RJ, Ridker PM. Anti-inflammatory therapy with canakinumab for the prevention of hospitalization for heart failure. *Circulation*. 2019;139:1289–1299. doi: 10.1161/CIRCULATIONAHA.118.038010
7. Marsh SA, Arthur HM, Spyridopoulos I. The secret life of nonclassical monocytes. *Cytometry A*. 2017;91:1055–1058. doi: 10.1002/cyto.a.23280
8. Epstein FH, Ross R. Atherosclerosis: an inflammatory disease. *N Engl J Med*. 1999;340:115–126.
9. Hansson GK. Inflammation, atherosclerosis, and coronary artery disease. *N Engl J Med*. 2005;352:1685–1695. doi: 10.1056/NEJMra043430
10. Libby P, Ridker PM, Hansson GK; Leducq Transatlantic Network on Atherothrombosis. Inflammation in atherosclerosis. *J Am Coll Cardiol*. 2009;54:2129–2138. doi: 10.1016/j.jacc.2009.09.009
11. Baylis RA, Gomez D, Mallat Z, Pasterkamp G, Owens GK. The CANTOS trial. *Arterioscler Thromb Vasc Biol*. 2017;37:e174–e177. doi: 10.1161/ATVBAHA.117.310097
12. Ridker PM, Everett BM, Thuren T, MacFadyen JG, Chang WH, Ballantyne C, Fonseca F, Nicolau J, Koenig W, Anker SD, et al; CANTOS Trial Group. Antiinflammatory therapy with canakinumab for atherosclerotic disease. *N Engl J Med*. 2017;377:1119–1131. doi: 10.1056/NEJMoa1707914
13. Cihakova D. Interleukin-10 stiffens the heart. *J Exp Med*. 2018;215:379–381. doi: 10.1084/jem.20180049
14. Ni S-H, Sun S, Huang Z-Y, Huang Y-S, Li H, Wang J-J, Xian S-X, Yang Z-Q, Wang L-J, Lu L. The pleiotropic association between IL-10 levels and CVD prognosis: evidence from a meta-analysis. *Cytokine*. 2019;119:37–46. doi: 10.1016/j.cyto.2019.02.017
15. Narasimhan PB, Marcovecchio P, Hamers AAJ, Hedrick CC. Nonclassical monocytes in health and disease. *Annu Rev Immunol*. 2019;37:439–456. doi: 10.1146/annurev-immunol-042617-053119
16. Frangogiannis NG. Regulation of the inflammatory response in cardiac repair. *Circ Res*. 2012;110:159–173. doi: 10.1161/CIRCRESAHA.111.243162
17. Swirski FK, Nahrendorf M. Cardioimmunology: the immune system in cardiac homeostasis and disease. *Nat Rev Immunol*. 2018;18:733–744. doi: 10.1038/s41577-018-0065-8
18. Bansal SS, Ismahil MA, Goel M, Patel B, Hamid T, Rokosh G, Prabhu SD. Activated T lymphocytes are essential drivers of pathological remodeling

in ischemic heart failure. *Circ Heart Fail*. 2017;10:e003688. doi: 10.1161/CIRCHEARTFAILURE.116.003688
19. Nahrendorf M, Swirski FK, Aikawa E, Stangenberg L, Wurdinger T, Figueiredo J-L, Libby P, Weissleder R, Pittet MJ. The healing myocardium sequentially mobilizes two monocyte subsets with divergent and complementary functions. *J Exp Med*. 2007;204:3037–3047. doi: 10.1084/jem.20070885
20. Auffray C, Fogg D, Garfa M, Elain G, Join-Lambert O, Kayal S, Sarnacki S, Cumano A, Lauvau G, Geissmann F. Monitoring of blood vessels and tissues by a population of monocytes with patrolling behavior. *Science*. 2007;317:666–670. doi: 10.1126/science.1142883
21. Chen YG, Satpathy AT, Chang HY. Gene regulation in the immune system by long noncoding RNAs. *Nat Immunol*. 2017;18:962–972. doi: 10.1038/ni.3771
22. Statello L, Guo C-J, Chen L-L, Huarte M. Gene regulation by long non-coding RNAs and its biological functions. *Nat Rev Mol Cell Biol*. 2021;22:96–118. doi: 10.1038/s41580-020-00315-9
23. Necsulea A, Soumillon M, Warnefors M, Liechti A, Daish T, Zeller U, Baker JC, Grützner F, Kaessmann H. The evolution of lncRNA repertoires and expression patterns in tetrapods. *Nature*. 2014;505:635–640. doi: 10.1038/nature12943
24. Boeckel J-N, Perret MF, Glaser SF, Seeger T, Heumüller AW, Chen W, John D, Kokot KE, Katus HA, Haas J, et al. Identification and regulation of the long non-coding RNA Heat2 in heart failure. *J Mol Cell Cardiol*. 2019;126:13–22. doi: 10.1016/j.yjmcc.2018.11.004
25. Ranzani V, Rossetti G, Panzeri I, Arrigoni A, Bonnal RJP, Curti S, Gruarin P, Provasi E, Sugliano E, Marconi M, et al. The long intergenic noncoding RNA landscape of human lymphocytes highlights the regulation of T cell differentiation by linc-MAF-4. *Nat Immunol*. 2015;16:318–325. doi: 10.1038/ni.3093
26. Wang P, Xue Y, Han Y, Lin L, Wu C, Xu S, Jiang Z, Xu J, Liu Q, Cao X. The STAT3-binding long noncoding RNA lnc-DC controls human dendritic cell differentiation. *Science*. 2014;344:310–313. doi: 10.1126/science.1251456
27. Zhang W, Zhao J, Deng L, Ishimwe N, Pauli J, Wu W, Shan S, Kempf W, Ballantyne MD, Kim D, et al. INKILN is a novel long noncoding RNA promoting vascular smooth muscle inflammation via scaffolding MKL1 and USP10. *Circulation*. 2023;148:47–67. doi: 10.1161/CIRCULATIONAHA.123.063760
28. Aghagolzadeh P, Plaisance I, Bernasconi R, Treibel TA, Quetglas CP, Wyss T, Wigger L, Nemir M, Sarre A, Chouvardas P, et al. Assessment of the cardiac noncoding transcriptome by single-cell RNA sequencing identifies FIXER, a conserved profibrogenic long noncoding RNA. *Circulation*. 2023;148:778–797. doi: 10.1161/CIRCULATIONAHA.122.062601
29. McDonagh TA, Metra M, Adamo M, Gardner RS, Baumbach A, Böhm M, Burri H, Butler J, Čelutkienė J, Chioncel O, et al; ESC Scientific Document Group. 2021 ESC guidelines for the diagnosis and treatment of acute and chronic heart failure. *Eur Heart J*. 2021;42:3599–3726. doi: 10.1093/eurheartj/ehab368
30. von Haehling S, Lainscak M, Doehner W, Ponikowski P, Rosano G, Jordan J, Rozentryt P, Rauchhaus M, Karpov R, Tkachuk V, et al. Diabetes mellitus, cachexia and obesity in heart failure: rationale and design of the Studies Investigating Co-morbidities Aggravating Heart Failure (SICA-HF). *J Cachexia Sarcopenia Muscle*. 2010;1:187–194. doi: 10.1007/s13539-010-0013-3
31. Fulster S, Tacke M, Sandek A, Ebner N, Tschope C, Doehner W, Anker SD, von Haehling S. Muscle wasting in patients with chronic heart failure: results from the Studies Investigating Co-morbidities Aggravating Heart Failure (SICA-HF). *Eur Heart J*. 2013;34:512–519. doi: 10.1093/eurheartj/ehs381
32. Schunk SJ, Triem S, Schmit D, Zewinger S, Sarakpi T, Becker E, Hütter G, Wrublewsky S, Küting F, Hohl M, et al. Interleukin-1α is a central regulator of leukocyte-endothelial adhesion in myocardial infarction and in chronic kidney disease. *Circulation*. 2021;144:893–908. doi: 10.1161/CIRCULATIONAHA.121.053547
33. Holzwirth E, Fischer-Schaepmann T, Obradovic D, von Lucadou M, Schwedhelm E, Daum G, Hindricks G, Marsche G, Trieb M, Thiele H, et al. Anti-inflammatory HDL effects are impaired in atrial fibrillation. *Heart Vessels*. 2022;37:161–171. doi: 10.1007/s00380-021-01908-w
34. Fuernau G, Beck J, Desch S, Eitel I, Jung C, Erbs S, Mangner N, Lurz P, Fengler K, Jobs A, et al. Mild hypothermia in cardiogenic shock complicating myocardial infarction. *Circulation*. 2019;139:448–457. doi: 10.1161/CIRCULATIONAHA.117.032722
35. Edgar R, Domrachev M, Lash AE. Gene Expression Omnibus: NCBI gene expression and hybridization array data repository. *Nucleic Acids Res*. 2002;30:207–210. doi: 10.1093/nar/30.1.207
36. Perez-Riverol Y, Bai J, Bandla C, García-Seisdedos D, Hewapathirana S, Kamatchinathan S, Kundu DJ, Prakash A, Frericks-Zipper A, Eisenacher M, et al. The PRIDE database resources in 2022: a hub for mass spectrometry-based proteomics evidences. *Nucleic Acids Res*. 2022;50:D543–D552. doi: 10.1093/nar/gkab1038
37. Abplanalp WT, John D, Cremer S, Assmus B, Dorsheimer L, Hoffmann J, Becker-Pergola G, Rieger MA, Zeiher AM, Vasa-Nicotera M, et al. Single-cell RNA-sequencing reveals profound changes in circulating immune cells in patients with heart failure. *Cardiovasc Res*. 2021;117:484–494. doi: 10.1093/cvr/cvaa101
38. Aran D, Looney AP, Liu L, Wu E, Fong V, Hsu A, Chak S, Naikawadi RP, Wolters PJ, Abate AR, et al. Reference-based analysis of lung single-cell sequencing reveals a transitional profibrotic macrophage. *Nat Immunol*. 2019;20:163–172. doi: 10.1038/s41590-018-0276-y
39. Tamura A, Hirai H, Yokota A, Kamio N, Sato A, Shoji T, Kashiwagi T, Torikoshi Y, Miura Y, Tenen DG, et al. C/EBPβ is required for survival of Ly6C− monocytes. *Blood*. 2017;130:1809–1818. doi: 10.1182/blood-2017-03-772962
40. Borrego F. The CD300 molecules: an emerging family of regulators of the immune system. *Blood*. 2013;121:1951–1960. doi: 10.1182/blood-2012-09-435057
41. Grage-Griebenow E, Lorenzen D, Fetting R, Flad HD, Ernst M. Phenotypical and functional characterization of Fc gamma receptor I (CD64)-negative monocytes, a minor human monocyte subpopulation with high accessory and antiviral activity. *Eur J Immunol*. 1993;23:3126–3135. doi: 10.1002/eji.1830231213
42. Lin MF, Jungreis I, Kellis M. PhyloCSF: a comparative genomics method to distinguish protein coding and non-coding regions. *Bioinformatics*. 2011;27:i275–i282. doi: 10.1093/bioinformatics/btr209
43. Wang L, Park HJ, Dasari S, Wang S, Kocher J-P, Li W. CPAT: Coding-Potential Assessment Tool using an alignment-free logistic regression model. *Nucleic Acids Res*. 2013;41:e74–e74. doi: 10.1093/nar/gkt006
44. Bazzini AA, Johnstone TG, Christiano R, Mackowiak SD, Obermayer B, Fleming ES, Vejnar CE, Lee MT, Rajewsky N, Walther TC, et al. Identification of small ORFs in vertebrates using ribosome footprinting and evolutionary conservation. *EMBO J*. 2014;33:981–993. doi: 10.1002/embj.201488411
45. Lee S, Liu B, Lee S, Huang S-X, Shen B, Qian S-B. Global mapping of translation initiation sites in mammalian cells at single-nucleotide resolution. *Proc Natl Acad Sci USA*. 2012;109:E2424–E2432. doi: 10.1073/pnas.1207846109
46. Wiśniewski JR, Zougman A, Nagaraj N, Mann M. Universal sample preparation method for proteome analysis. *Nat Methods*. 2009;6:359–362. doi: 10.1038/nmeth.1322
47. Grosche A, Hauser A, Lepper MF, Mayo R, von Toerne C, Merl-Pham J, Hauck SM. The proteome of native adult Müller glial cells from murine retina. *Mol Cell Proteomics*. 2016;15:462–480. doi: 10.1074/mcp.M115.052183
48. Vogl T, Tenbrock K, Ludwig S, Leukert N, Ehrhardt C, van Zoelen MAD, Nacken W, Foell D, van der Poll T, Sorg C, et al. Mrp8 and Mrp14 are endogenous activators of Toll-like receptor 4, promoting lethal, endotoxin-induced shock. *Nat Med*. 2007;13:1042–1049. doi: 10.1038/nm1638
49. Vogl T, Eisenblätter M, Völler T, Zenker S, Hermann S, van Lent P, Faust A, Geyer C, Petersen B, Roebrock K, et al. Alarmin S100A8/S100A9 as a biomarker for molecular imaging of local inflammatory activity. *Nat Commun*. 2014;5:4593. doi: 10.1038/ncomms5593
50. Vog T, Roth J, Sorg C, Hillenkamp F, Strupat K. Calcium-induced noncovalently linked tetramers of MRP8 and MRP14 detected by ultraviolet matrix-assisted laser desorption/ionization mass spectrometry. *J Am Soc Mass Spectrom*. 1999;10:1124–1130. doi: 10.1016/s1044-0305(99)00085-9
51. Heinz S, Benner C, Spann N, Bertolino E, Lin YC, Laslo P, Cheng JX, Murre C, Singh H, Glass CK. Simple combinations of lineage-determining transcription factors prime cis-regulatory elements required for macrophage and B cell identities. *Mol Cell*. 2010;38:576–589. doi: 10.1016/j.molcel.2010.05.004
52. Carlin LM, Stamatiades EG, Auffray C, Hanna RN, Glover L, Vizcay-Barrena G, Hedrick CC, Cook HT, Diebold S, Geissmann F. Nr4a1-dependent Ly-6Clow monocytes monitor endothelial cells and orchestrate their disposal. *Cell*. 2013;153:362–375. doi: 10.1016/j.cell.2013.03.010
53. Schunk SJ, Hermann J, Sarakpi T, Triem S, Lellig M, Hahm E, Zewinger S, Schmit D, Becker E, Möllmann J, et al. Guanidinylated apolipoprotein C3 (ApoC3) associates with kidney and vascular injury. *J Am Soc Nephrol*. 2021;32:3146–3160. doi: 10.1681/ASN.2021040503
54. Kapellos TS, Bonaguro L, Gemünd I, Reusch N, Saglam A, Hinkley ER, Schultze JL. Human monocyte subsets and phenotypes in major chronic inflammatory diseases. *Front Immunol*. 2019;10:2035. doi: 10.3389/fimmu.2019.02035
55. Lescoat A, Lecureur V, Roussel M, Sunnaram BL, Ballerie A, Coiffier G, Jouneau S, Fardel O, Fest T, Jégo P. CD16-positive circulating monocytes

and fibrotic manifestations of systemic sclerosis. *Clin Rheumatol*. 2017;36:1649–1654. doi: 10.1007/s10067-017-3597-6
56. Zimmermann HW, Seidler S, Nattermann J, Gassler N, Hellerbrand C, Zernecke A, Tischendorf JJW, Luedde T, Weiskirchen R, Trautwein C, et al. Functional contribution of elevated circulating and hepatic non-classical CD14+CD16+ monocytes to inflammation and human liver fibrosis. *PLoS One*. 2010;5:e11049. doi: 10.1371/journal.pone.0011049
57. Salvador P, Macías-Ceja DC, Gisbert-Ferrándiz L, Hernández C, Bernardo D, Alós R, Navarro-Vicente F, Esplugues JV, Ortiz-Masiá D, Barrachina MD, et al. CD16+ macrophages mediate fibrosis in inflammatory bowel disease. *J Crohns Colitis*. 2018;12:589–599. doi: 10.1093/ecco-jcc/jjx185
58. Thomas G, Tacke R, Hedrick CC, Hanna RN. Nonclassical patrolling monocyte function in the vasculature. *Arterioscler Thromb Vasc Biol*. 2015;35:1306–1316. doi: 10.1161/ATVBAHA.114.304650
59. Rabinovich A, Cohen JM, Cushman M, Wells PS, Rodger MA, Kovacs MJ, Anderson DR, Tagalakis V, Lazo-Langner A, Solymoss S, et al. Inflammation markers and their trajectories after deep vein thrombosis in relation to risk of post-thrombotic syndrome. *J Thromb Haemost*. 2015;13:398–408. doi: 10.1111/jth.12814
60. Du T, Tan Z. Relationship between deep venous thrombosis and inflammatory cytokines in postoperative patients with malignant abdominal tumors. *Brazilian J Med Biol Res*. 2014;47:1003–1007. doi: 10.1590/1414-431x20143695
61. Tsai S-Y, Segovia JA, Chang T-H, Morris IR, Berton MT, Tessier PA, Tardif MR, Cesaro A, Bose S. DAMP molecule S100A9 acts as a molecular pattern to enhance inflammation during influenza A virus infection: role of DDX21-TRIF-TLR4-MyD88 pathway. *PLoS Pathog*. 2014;10:e1003848. doi: 10.1371/journal.ppat.1003848
62. Holzinger D, Nippe N, Vogl T, Marketon K, Mysore V, Weinhage T, Dalbeth N, Pool B, Merriman T, Baeten D, et al. Myeloid-related proteins 8 and 14 contribute to monosodium urate monohydrate crystal–induced inflammation in gout. *Arthritis Rheumatol*. 2014;66:1327–1339. doi: 10.1002/art.38369
63. Lorey MB, Rossi K, Eklund KK, Nyman TA, Matikainen S. Global characterization of protein secretion from human macrophages following non-canonical caspase-4/5 inflammasome activation. *Mol Cell Proteomics*. 2017;16:S187–S199. doi: 10.1074/mcp.M116.064840
64. Wang J, Vodovotz Y, Fan L, Li Y, Liu Z, Namas R, Barclay D, Zamora R, Billiar TR, Wilson MA, et al. Injury-induced MRP8/MRP14 stimulates IP-10/CXCL10 in monocytes/macrophages. *FASEB J*. 2015;29:250–262. doi: 10.1096/fj.14-255992
65. Sprenkeler EGG, Zandstra J, van Kleef ND, Goetschalckx I, Verstegen B, Aarts CEM, Janssen H, Tool ATJ, van Mierlo G, van Bruggen R, et al. S100A8/A9 is a marker for the release of neutrophil extracellular traps and induces neutrophil activation. *Cells*. 2022;11:236. doi: 10.3390/cells11020236
66. Joshi A, Schmidt LE, Burnap SA, Lu R, Chan MV, Armstrong PC, Baig F, Gutmann C, Willeit P, Santer P, et al. Neutrophil-derived protein S100A8/A9 alters the platelet proteome in acute myocardial infarction and is associated with changes in platelet reactivity. *Arterioscler Thromb Vasc Biol*. 2022;42:49–62. 10.1161/ATVBAHA.121.317113
67. Marinković G, Koenis DS, de Camp L, Jablonowski R, Graber N, de Waard V, de Vries CJ, Goncalves I, Nilsson J, Jovinge S, et al. S100A9 links inflammation and repair in myocardial infarction. *Circ Res*. 2020;127:664–676. doi: 10.1161/CIRCRESAHA.120.315865
68. Wang S, Song R, Wang Z, Jing Z, Wang S, Ma J. S100A8/A9 in inflammation. *Front Immunol*. 2018;9:1298. doi: 10.3389/fimmu.2018.01298
69. Song R, Struhl K. S100A8/S100A9 cytokine acts as a transcriptional coactivator during breast cellular transformation. *Sci Adv*. 2021;7:eabe5357. doi: 10.1126/sciadv.abe5357
70. Wong KL, Tai JJ-Y, Wong W-C, Han H, Sem X, Yeap W-H, Kourilsky P, Wong S-C. Gene expression profiling reveals the defining features of the classical, intermediate, and nonclassical human monocyte subsets. *Blood*. 2011;118:e16–e31. doi: 10.1182/blood-2010-12-326355
71. Mattick JS, Amaral PP, Carninci P, Carpenter S, Chang HY, Chen L-L, Chen R, Dean C, Dinger ME, Fitzgerald KA, et al. Long non-coding RNAs: definitions, functions, challenges and recommendations. *Nat Rev Mol Cell Biol*. 2023;24:430–447. doi: 10.1038/s41580-022-00566-8
72. Luxán G, Dimmeler S. The vasculature: a therapeutic target in heart failure? *Cardiovasc Res*. 2021;118:53–64. doi: 10.1093/cvr/cvab047